MET exon 14 skipping mutation in non-small cell lung cancer; Diagnostic approach and clinicopathologic implications

Eun Kyung Kim

Department of Medicine

The Graduate School, Yonsei University

MET exon 14 skipping mutation in non-small cell lung cancer; Diagnostic approach and clinicopathologic implications

Directed by Professor Hyo Sup Shim

The Doctoral Dissertation
submitted to the Department of Medicine,
the Graduate School of Yonsei University
in partial fulfillment of the requirements for the degree
of Doctor of Philosophy

Eun Kyung Kim

December 2017

연세대학교
YONSEI UNIVERSITY

This certifies that the Doctoral Dissertation
of Eun Kyung Kim is approved.

Thesis Supervisor : Hyo Sup Shim

Thesis Committee Member #1 : Byoung Chul Cho

Thesis Committee Member #2 : Sun Hee Chang

Thesis Committee Member #3: Sangwoo Kim

Thesis Committee Member #4: Hye-Jeong Lee

The Graduate School
Yonsei University

December 2017

ACKNOWLEDGEMENTS

It is with great pleasure that I express my deep gratitude to my mentor and guide, Dr. H.S. Shim (Department of Pathology, Yonsei University College of Medicine). His inspiring, enthusiasm, meticulous scrutiny, scholarly advice, and scientific approach have been instrumental in helping me accomplish this task.

I also express sincere gratitude to Dr. B.C. Cho (Department of Internal Medicine, Yonsei University College of Medicine), Sangwoo Kim (Severance Biomedical Science Institute), Dr. S.H. Chang (Department of Pathology, Inje University Ilsan Paik Hospital), and Dr. H.J. Lee (Department of Radiology, Yonsei University College of Medicine). The guidance, suggestions, and constructive criticism from these individuals have greatly helped my scientific development and research.

I am deeply grateful to Kyung A Kim (Department of Pathology, Yonsei University College of Medicine) for important contributions to this research, specifically her meticulous and accurate experimental technique and analysis. I would also like to express my sincere gratitude to the Pathology Department of Yonsei University College of Medicine, which provided and encouraged a healthy research environment.

Finally, I am extremely thankful to my family and friends for their constant encouragement throughout this period of my research.

<TABLE OF CONTENTS>

LIST OF FIGURES

LIST OF TABLES

ABSTRACT

MET exon 14 skipping mutation in non-small cell lung cancer; Diagnostic approach and clinicopathologic implications

Eun Kyung Kim

Department of Medicine,
The Graduate School, Yonsei University

(Directed by Professor Hyo Sup Shim)

Recent studies revealed *MET* exon 14 skipping (*MET*ex14) as a driver mutation in non-small cell lung cancer (NSCLC). As *MET*ex14 is a biomarker that predicts the response of MET inhibitors, it is important for patient stratification. However, *MET*ex14 genomic alterations exhibit a highly diverse sequence composition, posing a challenge for clinical diagnostic testing. This study aimed to find a reasonable diagnostic assay for *MET*ex14 and identify its clinicopathologic implications and relationship with other genetic alterations in Korean NSCLC. We performed a comprehensive analysis of *MET*ex14 in 414 *EGFR/KRAS* mutation-negative and *ALK/ROS1* rearrangement-negative (quadruple negative) surgically resected NSCLC. We used real-time quantitative reverse transcription PCR (qRT-PCR), Sanger sequencing, and pyrosequencing for the first step, followed by next-generation sequencing (NGS; hybrid-capture targeted DNA/RNA sequencing) for PCR- or sequencing-positive cases. Clinicopathologic implications of the*MET*ex14 group were analyzed in a total of 880 NSCLCs. *MET*ex14 was confirmed in 13 patients (3.1%) by DNA- and RNA-NGS. After comparison of assay results, qRT-PCR and NGS demonstrated the highest concordance rate. The

mean supporting read (%) was 10.5% and 49% in DNA- and RNA- NGS, respectively. DNA-NGS revealed various lengths of deletions around and in exon 14. Moreover, *MET*ex14 was associated with adenocarcinoma or sarcomatoid carcinoma, old age, never smokers, and early stage of disease. No known oncogenic mutations or copy number variations were found other than the *TP53* mutation in two cases. Concurrent *MET* amplification was not observed and half of the cases showed *MET* overexpression. In summary, *MET*ex14 occurs in about 3% of NSCLCs and has characteristic clinicopathologic features. A classic DNA-based method can detect *MET*ex14, but sensitivity can be hampered by large deletions or low allele frequency. qRT-PCR, an mRNA-based method, is sensitive and specific and can be appropriate for screening *MET*ex14. When performing multiplex NGS panel testing, the gene panel should be designed to cover the genomic complexity of the *MET* gene to detect *MET*ex14.

Key words : *MET* exon 14 skipping, *MET* amplification, MET protein overexpression, non-small cell lung cancer, real time quantitative reverse transcription PCR, sanger sequencing, pyrosequencing, next generation sequencing

MET exon 14 skipping mutation in non-small cell lung cancer; Diagnostic approach and clinicopathologic implications

Eun Kyung Kim

Department of Medicine,
The Graduate School, Yonsei University

(Directed by Professor Hyo Sup Shim)

I. INTRODUCTION

Lung cancer is the leading cause of cancer-related death worldwide. Approximately 85–90% of lung cancers are characterized as non-small cell lung cancers (NSCLCs), and a considerable number present as locally advanced or metastatic disease. Molecularly targeted therapies have improved treatment for patients whose tumors harbor somatically activated oncogenes such as mutant *EGFR* or translocated *ALK*, *RET*, or *ROS1*[1]. However, the various molecular drivers of 24-36% of lung adenocarcinomas (ADCs)[2-5] and 37-60% of squamous cell carcinomas (SCCs)[6,7] remain unknown. Therefore, the identification of new driver mutations is critically important.

The hepatocyte growth factor receptor, encoded by the *MET* gene (*MET* proto-oncogene, located at chromosome7q21-q31), is a receptor tyrosine kinase that plays a fundamental role in regulating development and cell growth. Pathological activation of *MET*, through both gene copy-number amplification and point mutation, is a well-characterized driver of oncogenesis that occurs in several types of tumors. In cancer, *MET* activation promotes tumor proliferation, invasive growth, metastatic spread, and anti-apoptosis[8, 9].

MET overexpression is observed in 25-70% of NSCLCs and *MET* amplification in 2-11% of ADCs[2]. *MET* amplification has been implicated as one of the mechanisms of acquired resistance to anti-EGFR therapy[10, 11]. Several studies have

shown that an increased *MET* copy number is an independent negative prognostic factor in surgically resected NSCLC[12, 13]. Several clinical trials of MET-targeting agents for NSCLC patients with these features have revealed favorable results[14-17].

Recent studies[18, 19] reported that mutations of RNA splice acceptor and donor sites involving *MET* exon 14 could lead to exon skipping, resulting in an in-frame deletion of the juxtamembrane domain, which normally is a negative regulator of the kinase catalytic activities. More importantly, this type of mutations was mutually exclusive with other oncogenic drivers and showed partial responses to MET-targeted therapies. Somatic mutations affecting splice sites of *MET* exon 14 in primary lung cancer specimens and in a lung cancer cell line were published in the early 2000s[20-22]. Tyrosine 1003 (Y1003) in the juxtamembrane domain of MET is a binding site for c-Cbl, a ubiquitin protein ligase (E3), that causes ubiquitination, receptor endocytosis, and degradation of MET. Loss of *MET* exon14 maintains the reading frame and leads to increased MET stability and prolonged signaling upon hepatocyte growth factor stimulation, leading to increased oncogenic potential[23, 24].

MET exon14 skipping (*MET*ex14) alterations have been shown to occur in 3-4% of lung ADCs[2, 4, 5, 18, 19, 25] and in 2.3% of other lung neoplasms[19]. This frequency is comparable to that of *ALK* rearrangements; thus, identification of *MET*ex14 is important to apply appropriate target therapies. Additionally, *MET*ex14 has been reported to as a biomarker that predicts the response of MET inhibitors[18, 19]. However, *MET*ex14 alterations exhibit a highly diverse sequence composition, posing a challenge for diagnostic testing in clinics[19].

This study, aimed to find a reasonable diagnostic assay for *MET*ex14 and identify its clinicopathologic implications and relationship with other genetic alterations in Korean NSCLC patients.

II. MATERIALS AND METHODS

1. Clinical samples

The study cohort was retrospectively retrieved from the pathology archives. Formalin-fixed paraffin-embedded (FFPE) tumor tissues were obtained from

NSCLC patients who underwent surgical resection from January 2005 to January 2013 at Serverance Hospital, Korea. They were reviewed according to the 2015 WHO classification[26] and staged according to the 7th edition of the American Joint Committee on Cancer staging system[27, 28]. Demographic data and clinicopathologic characteristics were obtained from medical records. This retrospective study was approved by the institutional review board and was conducted in accordance with ethical guidelines and the Declaration of Helsinki.

Cohort 1 consisted of 91 *EGFR* mutation negative ADC cases, that were analyzed by real-time quantitative reverse transcription PCR (qRT-PCR), Sanger sequencing, and pyrosequencing. Not all analyses were performed for every case in cohort 1. Cohort 2 consisted of 323 *EGFR, KRAS, ALK,* and *ROS1* alteration-negative NSCLCs. All cases in cohort 2 were analyzed by qRT-PCR. Next generation sequencing (NGS) was also performed for cases that had positive results for one or more of the three tests (Figure 1). Cohort 3 consisted of 466 other driver mutation-positive or driver mutation-negative NSCLC cases and was used to compare clinicopathologic parameters with those of the *MET*ex14 group. The probes used for each test are shown in Table 1.

For smoking status, the patients were categorized as "never smokers" (had a lifetime exposure of ≤100 cigarettes), "former smokers" (have quit smoking for ≥12 months), and "current smokers" (currently smoking or have quit during the past 12 months)[29]. Follow-up duration was calculated from the surgical operation date to the last follow-up date (cut-off on May 31, 2017) or death. Overall survival (OS) was defined from the time of surgery to the time of cancer-related death. Meanwhile, disease free survival (DFS) was defined from the time of curative surgery to the time of radiological or pathological evidence of tumor relapse or progression.

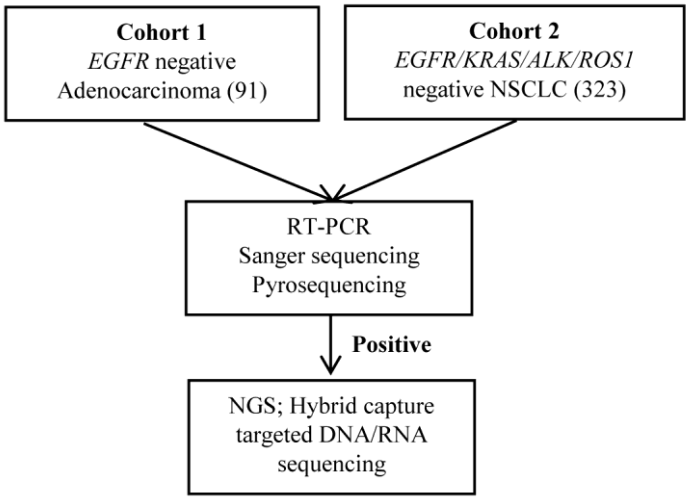

Figure 1. Experimental cohorts and diagnostic approach for *MET*ex14. Cohort 3 was composed of 466 other driver mutant-positive or driver mutant-negative cases of non-small cell lung cancer to enable comparison of their clinicopathologic parameters with those of the *MET*ex14 group.

Table 1. Primers used for each test

Methodology	No.	Position	Probe sequence
qRT-PCR		Forward for exon 13	5′-TGGGTTTTTCCTGTGGCTGAA-3′
		Reverse for exon 15	5′-GCATGAACCGTTCTGAGATGAATT-3′
		Overlapping an exon 13-15 junction	5′-AAGCAAATTAAAGATCAGTTTCC-3′
Sanger sequencing	1	116771720 116771739	tgtcgtcgattcttgtgtgc
		116771907 116771926	CACTTCGGGCACTTACAAGC
	2	116771778 116771797	cactgggtcaaagtctcctg
		116772035 116772055	caacaatgtcacaacccactg
	3	116771731 116771748	GTAAAACGACGGCCAGTcttgtgtgctgtcttata
		116771902 116771921	CGGGCACTTACAAGCCTATC
	4	116771918 116771936	CCCGAAGTGTAAGCCCAAC
		116772032 116772051	CAGGAAACAGCTATGACaatgtcacaacccactgagg
Pyrosequencing			Probe sequence
	5	Exon 13 and exon 14	5`-GTC GTC GAT TCT TGT GTG CTG TCT-3’ (Biotin) 5`-GGG CAC TTA CAA GCC TAT CCA AAT-3’
		Sequencing primer	5’ GGC CCA TGA TAG CCG 3’
	6	Exon 14 and exon 15	(Biotin) 5`-GCC GTC TTT AAC AAG CTC TTT-3’

		5`-TGT CAC AAC CCA CTG AGG TAT-3’
	Sequencing primer	5’-CTC AGA ACA ATA AAC TG-3’

qRT-PCR, real-time quantitative reverse transcription PCR

2. *MET* ex14 skipping

가. DNA and RNA preparations

FFPE tissue blocks were cut into five sections with 5μm thickness using a microtome. Genomic DNA extraction was performed using the ReliaPrep™ FFPE gDNAMiniprep System (Promega, WI, USA), while total RNA was isolated with the ReliaPrep™FFPE Total RNA Miniprep System (Promega). The concentration of genomic DNA and total RNA were measured using NanoDrop 1000 (Thermo-Scientific Inc.). Genomic DNA and RNA were stored at -80℃.

나. Real-time quantitative reverse transcription PCR (Real-time qRT-PCR)

To identify *MET* exon14 deletion, qRT-PCR was performed using the following primers: forward primer for exon 13 of *MET*, 5′-TGGGTTTTTCCTGTGGCTGAA-3′; reverse primer for exon 15 of *MET*, 5′-GCATGAACCGTTCTGAGATGAATT-3′; and probes overlapping an exon 13-exon 15 junction, 5′-AAGCAAATTAAAGATCAGTTTCC-3′[30]. TaqMan probes were labelled with the reporter dye molecule FAM (6-carboxyfluorescein) at the 5′ end and with TaqMan zip nucleic acid-4 black hole quencher-1 (ZNA-4-BHQ-1) probe at the 3’ end. The *GAPDH* gene (NM_001289746.1) was used as an endogenous control. We designed a forward primer (5’-CCTGCACCACCAACTGCTTAG-3’), reverse primer (5’-TGAGTCCTTCCACGATACCAA-3’) and probes (5’-6-FAM-CCCT GGCCAAGGTCATCCATGA-BHQ-1-3’). With the SensiFAST Probe Lo-ROX One-Step Kit (Bioline), 10μM primers (forward and reverse) each at 0.5μL, a 10μM TaqMan probe at 0.25μL, and 50ng RNA were mixed in a total reaction volume of 10μL. PCR conditions were 45℃ for 20min, and 95℃ for 10 min followed by 40 cycles of amplification at 95℃ for 15s and 60℃ for 30s on the ABI 7500 Real-Time PCR Detection System (Applied Biosystems).

Threshold cycle (Ct) values of < 34 were considered as *MET*ex14 positive, and ≥ 34 as *MET*ex14 negative. All experiments were performed in triplicate for consistency.

다. Sanger sequencing

For Sanger sequencing, we amplified 100ng of genomic DNA and created several probes to sequence exon 14 and its vicinity as fully as possible, as shown in Table 1.The PCR products were analyzed by electrophoresis and purified using the QIAquick PCR Purification Kit (Qiagen, CA, USA). Each PCR products was sequenced with each forward or reverse primer. The PCR cycling parameters used were as follows: 94℃ for 2 min; 35 cycles of (94℃ for 20 s, 59℃ for 10 s, and 72℃ for 30 s); 72℃ for 5 min; and 4℃ hold. PCR products were checked on a 2% agarose gel.

라. Pyrosequencing

One hundred nanograms of genomic DNA was amplified in a 20-μl reaction with Maxime PCR PreMix [i-StarTaq^{TM} GH]. To amplify exon 13 and exon 14, the forward primer 5` GTC GTC GAT TCT TGT GTG CTG TCT 3’ and the reverse primer (Biotin) 5` GGG CAC TTA CAA GCC TAT CCA AAT 3’ were used. The sequencing primer used was 5’ GGC CCA TGA TAG CCG 3’. To amplify exon 14 and exon 15, the forward primer (Biotin) 5` GCC GTC TTT AAC AAG CTC TTT 3’ and the reverse primer 5` TGT CAC AAC CCA CTG AGG TAT 3’ were used. The sequencing primer used was 5’ CTC AGA ACA ATA AAC TG 3’ (Table 1). The PCR cycling parameters were the same as those used for Sanger sequencing. Sequencing was performed on a PyroMark Q24 instrument (Qiagen) according to the manufacturer’s protocol.

마. Next generation sequencing (NGS); hybrid capture targeted DNA/RNA sequencing

A customized hybrid capture–based assay encompassing 46 genes for DNA and 18 genes for RNA was used. Synthetic DNA and RNA probes were

designed to capture all protein-coding exons of target genes. We used the QiagenAllPrep DNA/RNA FFPE Kit (Qiagen, CA, USA) following the manufacturer's instructions to extract FFPE-DNA and –RNA. The input amounts of extracted DNA and RNA were 100-1000ng/50μL and 50-100ng/5μL, respectively. Genomic DNA was fragmented to 150-250bp using a Covaris E Series instrument (Covaris, MA, USA). Libraries were constructed using the NEBNext® Ultra™ II DNA/RNA Library Prep Kit for Illumina (New England Biolabs, MA, USA) through a series of enzymatic steps including end-repair, adaptor ligation, size selection and PCR enrichment. Hybrid capture selection was performed using Dynabeads® M-270 Streptavidin (Life Technologies, CA, USA) and KAPA HiFiHotStartReadyMix (Kapa Biosystems, MA, USA). Sequencing of the libraries was carried out on a MiSeq (Illumina, CA, USA) according to the manufacturer's protocol ("Preparing libraries for sequencing on the MiSeq", October 2013). A final library concentration ranging from 8 to 10pM was used to carry out cluster generation and sequencing on a standard flow cell and 300-cycle MiSeq Reagent Kit v3 (150x150). Tumor samples were sequenced to a target depth of coverage more than 300x (DNA) and 1000x (RNA).

Sequencers were monitored by an automated data management system, which initiates the analysis pipeline upon the end of the sequencing run. DNA sequences were mapped to the human genome hg19 using BWA-MEM software[31]. We modified the mapping information using IndelRealigner and BaseRecalibrator provided by GATK (https://software.broadinstitute.org/gatk) and removed duplicated reads using Picard software (http://broadinstitute.github.io/picard/). We explored SNV and INDEL variants using FreeBayes software and annotated mutation information using ANNOVAR software. The copy number for each gene was set to 2N as the median coverage for the entire target area. Based on this, the coverage of the entire target area was converted into the number of DNA copies and expressed as a boxplot for each gene. RNA sequences were mapped to the human genome hg19 using STAR software[32]. For fusion gene searches, we used STAR-Fusion,

FusionCatcher, and In-house software[33, 34]. We searched for empty RNA read between exon 13 and exon 15 to find *MET*ex14. The amount of gene expression was normalized to the transcript length in the sample using StringTie software[35]. R package edgeR was used to standardize the expression level between samples[36].

3. MET amplification and protein expression

가. Construction of tissue microarray

The tumor area on the FFPE tissue block was marked on the hematoxylin and eosin-stained section. Three representative 2-mm cores were obtained from each tumor and sectioned by 4-μm thickness for silver in situ hybridization (SISH), fluorescence in situ hybridization (FISH), and immunohistochemistry (IHC).

나. Silver in situ hybridization (SISH)

MET gene copy number was analyzed using bright-field microscopy and SISH technology. Probing was carried out using both *MET*-specific and centromere 7 (*CEP7*)-specific probes according to the manufacturer's protocols (Ventana Medical Systems). The assessment of gene copy number was performed independently and blinded from IHC. The scoring was carried out in 50 non-overlapping nuclei per core in regions identified by optical analysis of tissue sections as having higher gene copy number. The following data were recorded for each sample: mean *MET* gene and mean *CEP7* copy number per cell and *MET/CEP7* ratio. The core with the highest average *MET* gene copy number per cell was selected. Small clusters were scored as 6 signals, and big clusters as 12 signals, similar to *HER2* breast cancer practice[37].

다. Immunohistochemistry (IHC)

FFPE tissues were stained using the Ventana automated immunostainerBenchMark XT (Ventana Medical Systems, Tucson, AZ, USA). The slides were dried at 60℃ for 1 h and deparaffinized using EZ Prep

(Ventana Medical Systems) at 75℃ for 4 min. Cell conditioning was performed using CC1 solution (Ventana Medical Systems) at 100℃ for 64 min.

c-MET (SP44) rabbit monoclonal primary antibody (catalog 7904430; Ventana Medical Systems, Tucson, AZ), ALK (rabbit monoclonal, clone D5F3; Cell Signaling Technology, Danvers, MA, USA), and ROS1 (rabbit monoclonal, clone D4D6; Cell Signaling Technology) antibodies were diluted to 1:50, treated, and incubated at 37℃ for 32 min. Signals were detected using the OptiView DAB IHC Detection Kit (Ventana Medical Systems). Counter staining was performed with Hematoxylin I (Ventana Medical Systems) for 4 min at room temperature. Thyroid transcription factor-1 (TTF-1, 8G7G3/1, monoclonal, 1:500; nuclear staining; Ventana) and p40 (rabbit, polyclonal, 1:2000; nuclear staining; Oncogene, Cambridge, MA) staining were also performed according to the manufacturer's instruction to confirm histological sub-classification.

Membranous and/or cytoplasmic reactivity was assessed using an H-score method, which calculates the sum of the products of multiplying intensity (0, 1, 2, and 3) by extent of each staining area (%). Intensity was defined as follows: 0 for no detectable staining, 1+ for weak reactivity mainly detectable at high magnification (20-40x objective), and 2+ or 3+ for more intense (moderate or strong, respectively) reactivity easily detectable at low magnification (4x objective). The c-MET positivity was defined asH-score of 100 or more[17, 38]. ALK and ROS1 positivity were defined as an H-score of ≥100, extent of ≥75%, or the presence of 2+ or 3+ intensity[39]. Cases showing positive in IHC were confirmed by FISH.

4. *EGFR* mutation; Peptide nucleic acid-locked nucleic acid polymerase chain reaction (PNA-LNA PCR) clamp

Peptide nucleic acid-locked nucleic acid polymerase chain reaction (PNA-LNA PCR) clamp PNAClamp™ EGFR Mutation Detection Kit (Panagene, Inc., Daejeon, Korea)[40, 41] was used to detect *EGFR* mutations in real-time PCR.

All reactions were done in 20μL volumes using template DNA, primer and PNA probe set, and SYBR Green PCR Master Mix. All reagents were included in the kit. Real-time PCR was performed using a CFX 96 detection system (Bio-Rad, USA). PCR cycling commenced with a 5 min hold at 94℃ followed by 40 cycles of 94℃ for 30s, 70℃ for 20s, 63℃ for 30s, and 72℃ for 30s. Detection of each of 29 mutations in the *EGFR* gene was possible with the PNAClamp detection kit. The efficiency of PCR clamping was determined by measuring the Ct value. Ct values for the control and mutation assays were obtained by observing the SYBR Green amplification plots. The delta Ct (ΔCt) value was calculated (control Ct−sample Ct), ensuring that the sample and control Ct values were from the test and wild type control samples. The cut-off ΔCt was defined as 2.

5. *ALK* and *ROS1* fusion; Fluorescence in situ hybridization (FISH)

A break-apart *ALK* or *ROS1* probe (Vysis LSI Dual Color, Break Apart Rearrangement Probe; Abbott Molecular, Abbot Park, IL, USA) was used according to the manufacturer's instructions. *ALK* or *ROS1* rearrangements were recognized as positive when more than 15% of tumor cells display split signals (two or more signal diameters apart) or isolated signals containing a kinase domain (green for *ROS1* and red for *ALK*)[42, 43].

6. Analysis of TCGA data and published papers

To retrieve the published characteristics of *MET*ex14, we analyzed the public database cBioPortal (http://www.cbioportal.org) for Cancer Genomics[44, 45]. We also assessed papers published in English above the level of case reports.

7. Statistical analysis

Statistical analysis was performed to analyze associations of mutation, protein expression and gene copy number with clinical characteristics using Pearson's chi square test and Fisher's exact test. The Kaplan–Meier method was used to estimate the survival rates of the different groups. The equivalences of the survival curves were tested by log-rank statistics. The Cox proportional hazards

model was employed for univariate and multivariate survival analyses. Statistically significant variables found in the univariate survival analysis were evaluated in the multivariate survival analysis. All results with a two-sided *P*-value of <0.05 were considered significant. Statistical calculations were performed using the statistical package SPSS 21.0 (IBM Corp., Armonk, NY).

III. RESULTS

1. Diagnostic approach and genetic features of *MET*ex14

We first conducted qRT-PCR, Sanger sequencing, and pyrosequencing in cohorts 1 and 2. Using these results, we confirmed the *MET*ex14-positive cases by NGS. The qRT-PCR method showed the highest sensitivity (100%) and specificity (66.7%), (Table 2; Figures 2 and 3). A *KRAS* mutation (Q61H) was revealed by NGS in one PCR(+)/NGS(-) case. Five cases showed discrepancies between the Sanger sequencing and NGS results. Among them, three cases had large deletions (237, 335, and 737 base pairs). The other two had low DNA variant allele frequency (VAF; 1 % and 6%).

Table 2. Correlation between qRT-PCR, Sanger sequencing, pyrosequencing, and NGS in cases tested by all three assays

Methodology (No. of cases)	Results (No.)	NGS (16)		p-value	Sensitivity (%)	Specificity (%)
		*MET*ex14	Wild			
qRT-PCR	*MET*ex14 (14)	13	1	0.025	100.0	66.7
(414)	Wild (400)	0	2			
Sanger sequencing	*MET*ex14 (8)	8	0	0.200	61.5	100.0
(102)	Wild (94)	5	3			
Pyrosequencing	*MET*ex14 (4)	2	2	0.429	33.3	0
(77)	Wild (73)	4	0			

qRT-PCR, real-time quantitative reverse transcription PCR; NGS, next-generation sequencing.

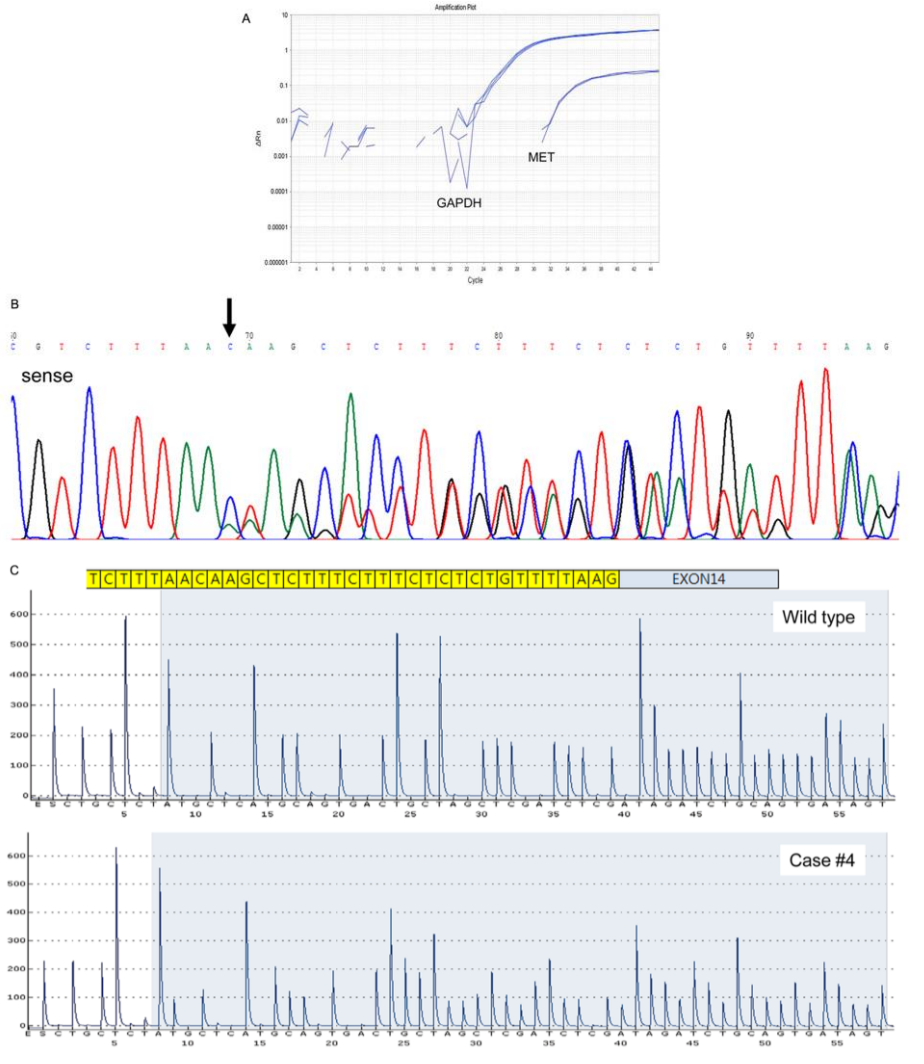

Figure 2. Results of case #4 (23bp deletion). Each test showed consistent results. A. qRT-PCR shows amplification curves (Ct=32.38), B. Sanger sequencing shows deletion (arrow; starting point), C. Pyrosequencing shows deletion, D. Coverage plot and integrative genomics viewer (IGV) of next generation sequencing (NGS); DNA-NGS shows deletion on intron 13. E. Coverage plot and IGV of NGS; RNA-NGS shows absence of exon 14 between exon 13 and exon 15.

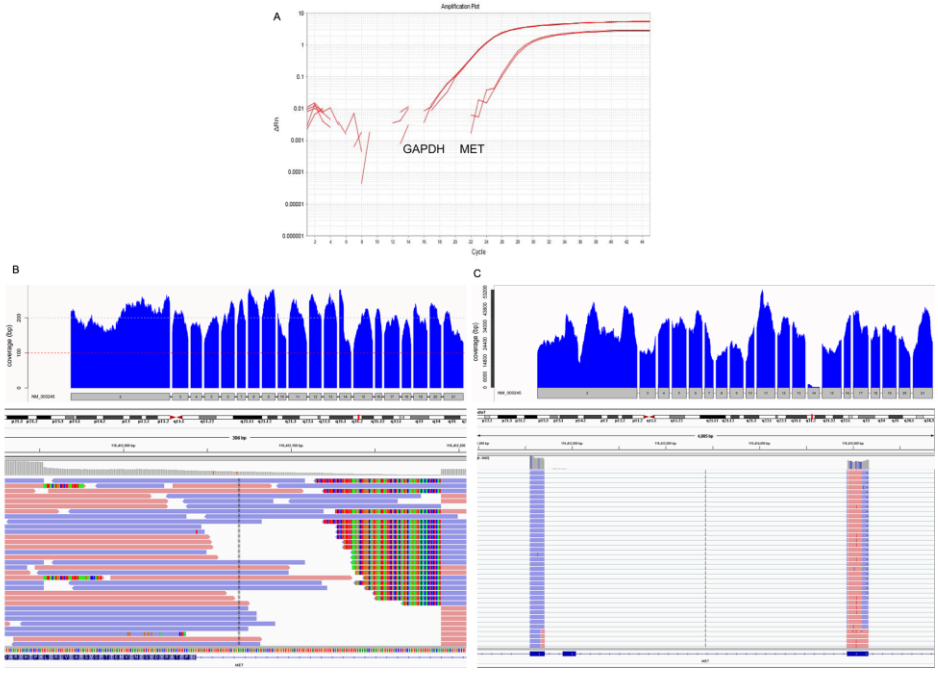

Figure 3. Results of case #13 (237bp deletion). *MET*ex14 was not detected in

Sanger sequencing and pyrosequencing. A. qRT-PCR (Ct=26.2), B. Coverage plot and integrative genomics viewer (IGV) of next generation sequencing (NGS); DNA-NGS shows large deletions involving exon 14 and intron 14. C. Coverage plot and IGV of NGS; RNA-NGS shows absence of exon 14 between exon 13 and exon 15.

Most mutations were deletion, which occurred at splice donor or acceptor, and two cases caused whole exon 14 deletion (Table 3 and Figure 4). The mean VAF of DNA and RNA sequencing were 10.5% and 49.0%. Accompanying other genetic alterations were described in Table 4. Two cases (15.4%) had *TP53* mutation that has been known to be likely oncogenic in NSCLC. No coexisting driver mutations or known oncogenic copy number alterations in NSCLC were observed.

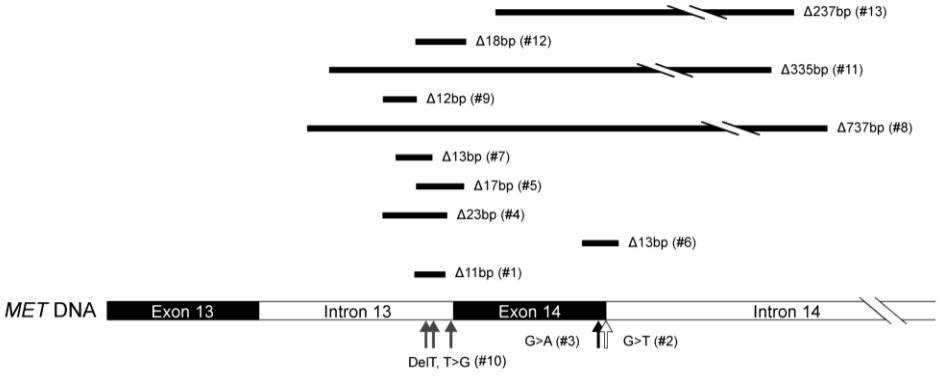

Figure 4. Genomic position of *MET*ex14 alterations (# case number). DNA sequencing revealed various lengths of indel around and in exon 14.

Table 3. Summary of *METex14* alterations (Chr7; NM_000245.2)

Case no.	*METex14* alterations (gDNA/cDNA/Protein)	Types of alteration	VAF (%)		qRT-PCR	Sanger sequencing	Pyrosequencing
			DNA	RNA			
1	g.116411891_116411901del11 / c.2888-12_2888-3delCTCTGTTTTAAinsT / -	Indel splice acceptor	17.5 (14/80)	53.9 (5311/9850)	Deletion	Deletion	Deletion
2	g.116412044G>T / c.3028+1G>T / -	Base substitution splice donor	15.2 (23/151)	40.5 (2424/5982)	Deletion	Substitution	Wild
3	g.116412043G>A / c.3028G>A / p.D1010N	Base substitution splice donor	14.9 (16/107)	66.1 (6220/9414)	Deletion	Substitution	Wild
4	g.116411875_116411897del23 / c.2888-28_2888-6delCAAGCTCTTTCTTTCTCTCTGTTinsA / -	Indel splice acceptor	15.0 (35/233)	73.9 (17437/23564)	Deletion	Deletion	Deletion
5	g.116411889_116411905del17 / c.2888-14_2900delCTCTCTGTTTTAAGATC / -	Indel splice acceptor	5.5 (16/293)	47.8 (8865/18545)	Deletion	Deletion	-
6	g.116412033_116412045del13 / c.3018_3028+2delTTTTCCAGAAGGT / -	Indel splice donor	6.2 (10/161)	21.3 (832/3898)	Deletion	Wild	-
7	g.116411885_116411897del13 / c.2888-19_2888-8delTCTTTCTCTCTGTinsG / -	Indel splice acceptor	18.5 (56/302)	60.2 (8238/13693)	Deletion	Deletion	-
8	g.116411748_116412484del737 / c.2887+40_3028+441del / -	Whole exon 14 deletion	2.3 (3/133)	24 (1258/5267)	Deletion	Wild	-
9	g.116411876_116411887del12 / c.2888-27_2888-16delAAGCTCTTTCTT / -	Indel splice acceptor	1.0 (4/372)	27.7 (2677/9640)	Deletion	Wild	-
10	g.116411894_116411896delinsGG / c.2888-9_2888-7delinsGG / -	Indel/base substitution splice acceptor	11.3 (35/310)	58.1 (4353/7493)	Deletion	Deletion	-
11	g.116411758_116412092del335 / c.2887+50_3028+49del/ -	Whole exon 14 deletion	1.0 (2/198)	14.1 (1199/8490)	Deletion	Wild	-
12	g.116411885_116411903del19 / c.2888-18_2888-1delCTTTCTCTCTGTTTTAAG / -	Indel splice acceptor	3.9 (4/101)	72.4 (8989/12410)	Deletion	Deletion	Wild
13	g.116411953_116412189del237 / c.2938_3028+146del / -	Indel splice donor	26.8 (62/231)	76.7 (20810/27116)	Deletion	Wild	Wild

gDNA, genomic DNA; cDNA, complementary DNA; VAF, variant allele frequency; qRT-PCR, real-time quantitative reverse transcription PCR.

Table 4. Other genetic alterations accompanied by *MET*ex14

Case no.	Histology	*MET* amplification[1]	MET overexpression[2] (H-score)	Other somatic mutations	Copy number alterations
1	ADC	None[3]	None (90)	***TP53* R306**[4], *NTRK3* K346N	None
2	ADC	None[3]	None (20)	None	None
3	ADC	None[3]	Present (150)	***TP53* P152L, TP53 R248Q, TP53 S183**, *CD274* E164K, *EGFR* P733S, *RB1* R661W	None
4	ADC	None	N/A	None	None
5	ADC	None	Present (140)	None	None
6	ADC	None	N/A	None	None
7	ADC	None	Present (100)	None	None
8	ADC	None	N/A	None	None
9	ADC	None	N/A	None	None
10	ADC	None	None (90)	*ALK* K1491R, *ALK* D1529E	None
11	ADC	None	N/A	None	None
12	SC	None	Present (100)	*AKT1* F35L, *DDR2* R124L,*NTRK1* R85C,*NTRK3* K346N, *RET* V757M, *SMARCA4* E861K	None
13	SC	None	None (90)	*JAK3* A127D,*NTRK2* E745*, *NTRK3* V799L, *SMARCA4* S266L	None

[1]These cases were evaluated by next generation sequencing.

[2] MET protein overexpression denotes an H-score of ≥100.

[3]These cases were also evaluated by silver in situ hybridization. *MET* amplification denotes a *MET/CEP17* ratio of ≥2.0 or an average *MET* copy number of ≥6.0 signals/cell.

[4]Bold type indicates "likely oncogenic mutation" (http://www.cbioportal.org).

ADC, adenocarcinoma; SC, sarcomatoid carcinoma; N/A, Not applicable

2. Clinicopathologic features of *MET*ex14 NSCLC

Cohort 1 and 2 consisted of 230 ADCs, 105 SCCs, 33 mucinous adenocarcinomas, 21 sarcomatoid carcinomas (SCs), 15 large cell carcinomas, 2 adenosquamous carcinomas, 7 carcinoid tumors, and 1 colloid adenocarcinoma. *MET*ex14 was found in 3.14% of cohort 1 and 2 (13/414; Table 5). The histologic type was ADC (4.8%; 11/230) and SC (9.5%; 2/21; Figure 5). The predominant subtype was acinar or lepidic in ADCs. Two SC consisted of spindle cells admixed with a solid adenocarcinomatous component. Moderate to marked lymphocytic infiltration with or without lymphoid follicle formation was found in seven cases (53.8%).

Table 5. Clinicopathologic features of *MET*ex14 NSCLCs

Case No.	Age	Gender	Smoking (pack-years)	Histology	Subtype	Stage	OS (mo)
1	54	M	Never	ADC	Acinar	IIA	10.1
2	71	F	Never	ADC	Acinar	IB	84.8
3	69	M	Current (25)	ADC	Acinar	IA	78.3+
4	71	M	Ex-smoker (40)	ADC	Lepidic	IA	31.5+
5	73	M	Current (25)	ADC	Acinar	IA	15.2+
6	72	M	Never	ADC	Lepidic	IA	20.7+
7	71	F	Never	ADC	Lepidic	IA	14.7+
8	64	F	Never	ADC	Acinar	IA	9.7+
9	68	F	Never	ADC	Lepidic	IA	6.6+
10	79	M	Never	ADC	Acinar	IB	11.0+
11	58	F	Never	ADC	Lepidic	IB	6.7
12	80	F	Never	SC	ADC + spindle	IB	15.7+
13	69	M	Ex-smoker (60)	SC	ADC + spindle	IIB	12.7+

NSCLC, non-small cell lung cancer; OS, overall survival; M, male; F, female; ADC, adenocarcinoma; SC, sarcomatoid carcinoma

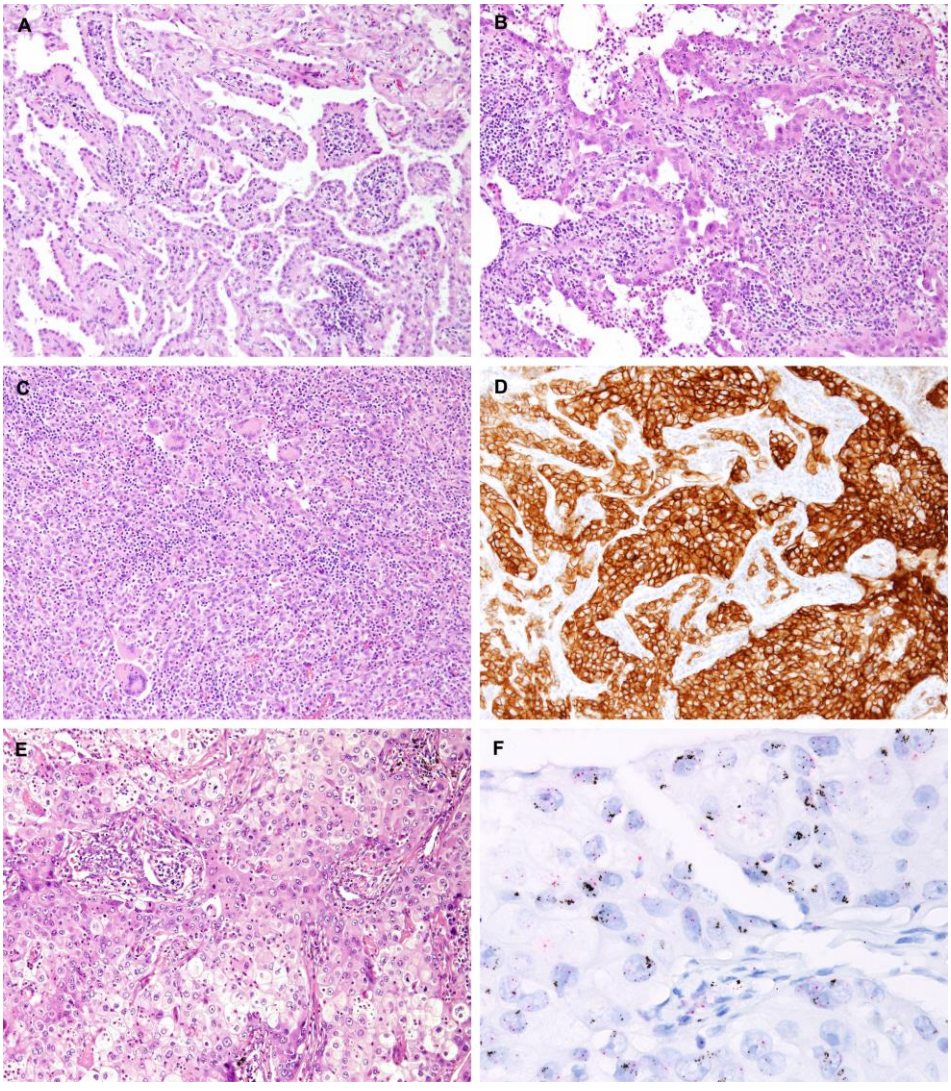

Figure 5. Representative photos of *MET*ex14, MET overexpression, and *MET* amplification. A. Lepidic predominant adenocarcinoma with mild lymphocytic infiltration, B. acinar predominant adenocarcinoma with moderate lymphocytic infiltration, C. sarcomatoid carcinoma with marked lymphocytic infiltration, D. MET immunohistochemical stain showing overexpression (H-score = 300), and E. sarcomatoid carcinoma with *MET* amplification demonstrated by MET SISH (F. *MET/CEP7* ratio 7.24 and average *MET* copy number 15.68).

In cohort 1 and 2 (Table 6), *MET*ex14 appeared more frequently in never

smokers (*P*=0.019), lepidic subtype (*P*=0.002), and early stage (*P*=0.033). When compared with other driver mutation-positive groups and all-negative groups including cohort 3 (n=880; Table 7 and Figure 6), the *MET*ex14 group revealed correlations with old age (*P*=0.022), females (*P*<0.001), never smokers (*P*<0.001), ADCs and SCs (*P*<0.001), lepidic subtype (*P*<0.001), and early stage (*P*<0.001).

Table 6. *MET*ex14 in cohorts 1 and 2.

		*MET*ex14-positive n = 13 (3.1)	*MET*ex14-negative n = 401 (96.9)	p-value
Age	Median	71	66	0.124
	≤ 60	2 (15.4)	114 (28.4)	0.530
	> 60	11 (84.6)	287 (71.6)	
Gender	Male	7 (53.8)	291 (72.6)	0.205
	Female	6 (46.2)	110 (27.4)	
Smoking	Never smoker	9 (69.2)	118 (29.4)	0.019
	Ex-smoker	2 (15.4)	151 (37.7)	
	Current smoker	2 (15.4)	132 (32.9)	
Histology	ADC	11 (84.6)	219 (54.6)	0.309
	SCC	0 (0)	105 (26.2)	
	MC	0 (0)	33 (8.2)	
	SC	2 (15.4)	19 (4.7)	
	LCC	0 (0)	15 (3.7)	
	ASC	0 (0)	2 (0.5)	
	CC	0 (0)	1 (0.2)	
	CT	0 (0)	7 (1.7)	
Subtype	Lepidic	5 (45.5)	23 (10.4)	0.002
	Acinar	6 (54.5)	114 (51.4)	
	Papillary	0 (0)	27 (12.2)	
	Solid	0 (0)	47 (21.2)	
	Micropapillary	0 (0)	11 (5.0)	
Stage	I	11 (84.6)	219 (54.6)	0.033
	II	2 (15.4)	96 (23.9)	
	III	0 (0)	72 (18.0)	
	IV	0 (0)	14 (3.5)	

ADC, adenocarcinoma; SCC, squamous cell carcinoma; MC, mucinous adenocarcinoma; SC, sarcomatoid carcinoma; LCC, large cell carcinoma; ASC, adenosquamous carcinoma; CC, colloid adenocarcinoma; CT, carcinoid tumor

Table 7. Comparison of *MET*ex14 and other mutation positive/negative groups

N (%)	Total 880 (100)	*MET*ex14 13 (1.5)	*EGFR* 382 (43.4)	*KRAS* 31 (3.5)	*ALK* 29 (3.3)	*ROS1* 8 (0.9)	All negative 417 (47.4)	*P*-value
Age (yrs)								0.022
≤ 60	309 (35.1)	2 (15.4)	150 (39.3)	11 (35.5)	16 (55.2)	4 (50.0)	126 (30.2)	
> 60	571 (64.9)	11 (84.6)	232 (60.7)	20 (64.5)	13 (44.8)	4 (50.0)	291 (69.8)	
Gender								<0.001
Male	487 (55.3)	7 (53.8)	144 (37.7)	20 (64.5)	14 (48.3)	3 (37.5)	299 (71.7)	
Female	393 (44.7)	6 (46.2)	238 (62.3)	11 (35.5)	15 (51.7)	5 (62.5)	118 (28.3)	
Smoking								<0.001
Never smoker	439 (49.9)	9 (62.2)	271 (70.9)	12 (37.8)	15 (51.7)	6 (75.0)	126 (30.2)	
Ex-smoker	254 (28.9)	2 (15.4)	81 (21.2)	8 (25.8)	8 (27.6)	0 (0)	155 (37.2)	
Current smoker	187 (21.3)	2 (15.4)	30 (7.9)	11 (35.5)	6 (20.7)	2 (25.0)	136 (32.6)	
Histology								<0.001
Adenocarcinoma	671 (76.3)	11 (84.6)	375 (98.2)	18 (58.1)	29 (100.0)	8 (100.0)	230 (55.2)	
Squamous cell ca	107 (12.2)	0 (0)	0 (0)	0 (0)	0 (0)	0 (0)	107 (25.7)	
Mucinous ca	45 (5.1)	0 (0)	0 (0)	11 (35.5)	0 (0)	0 (0)	34 (8.2)	
Sarcomatoid ca	24 (2.7)	2 (15.4)	1 (0.3)	1 (3.2)	0 (0)	0 (0)	20 (4.8)	
Large cell ca	18 (2.0)	0 (0)	1 (0.3)	1 (3.2)	0 (0)	0 (0)	16 (3.8)	
Adenosquamous ca	7 (0.8)	0 (0)	5 (1.3)	0 (0)	0 (0)	0 (0)	2 (0.5)	
Colloid ca	1 (0.1)	0 (0)	0 (0)	0 (0)	0 (0)	0 (0)	1 (0.2)	
Carcinoid tumor	7 (0.8)	0 (0)	0 (0)	0 (0)	0 (0)	0 (0)	7 (1.7)	
Subtype								<0.001
Lepidic	96 (13.8)	5 (45.5)	61 (16.1)	7 (22.6)	0 (0)	0 (0)	23 (9.7)	
Acinar	380 (54.8)	6 (54.5)	219 (57.8)	14 (45.2)	18 (64.3)	5 (62.5)	118 (49.8)	
Papillary	86 (12.4)	0 (0)	52 (13.7)	0 (0)	3 (10.7)	1 (12.5)	30 (12.7)	
Solid	86 (12.4)	0 (0)	21 (5.5)	6 (19.4)	5 (17.9)	1 (12.5)	53 (22.4)	
Micropapillary	46 (6.6)	0 (0)	26 (6.9)	4 (12.9)	2 (7.1)	1 (12.5)	13 (5.5)	
Stage								<0.001
I	542 (61.6)	11 (84.6)	272 (71.2)	17 (54.9)	17 (58.6)	3 (37.5)	222 (53.2)	
II	158 (18.0)	2 (15.4)	44 (11.5)	9 (29.0)	3 (10.3)	1 (12.5)	99 (23.7)	
III	149 (16.9)	0 (0)	54 (14.1)	3 (9.7)	8 (27.6)	3 (37.5)	81 (19.4)	
IV	31 (3.5)	0 (0)	12 (3.1)	2 (6.5)	1 (3.4)	1 (12.5)	15 (3.6)	

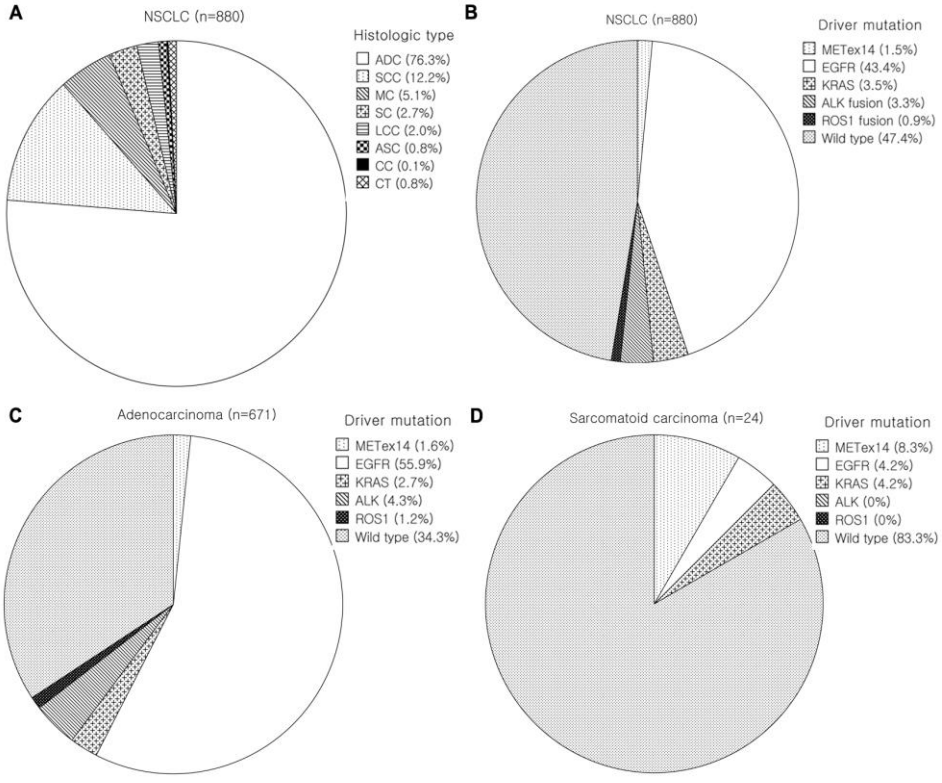

Figure 6. Histologic types and driver mutations in NSCLC. A and B. NSCLC, C. adenocarcinoma, and D. sarcomatoid carcinoma.

3. Correlation between *MET* amplification and protein overexpression

The *MET* SISH and IHC results were not correlated with *MET*ex14 (Table 8 and Figure 5). *MET*-amplified NSCLCs were found in 3.8% of the cases (13/338). These tumors were associated with higher cancer stage (P=0.014) and were more frequent in SCs and large cell carcinomas (P=0.028; Table 9). MET overexpression appeared in 44.2% (226/511) of the tumors and were mainly found in early stage cases (P<0.001). These tumors were mainly composed of ADCs and tended to be mucinous adenocarcinoma (P=0.012; Table 9).

Table 8. Correlation between *MET*ex14, *MET* amplification, and MET protein overexpression

SISH and IHC	*MET*ex14-positive (%)	*MET*ex14-negative (%)	Total	p-value
Ratio				> 0.999
< 2	4 (100.0)	321 (96.1)	325	
≥ 2	0 (0)	13 (3.9)	13	
Copy number				> 0.999
< 6	5 (100.0)	333 (98.5)	338	
≥ 6	0 (0)	5(1.5)	5	
H-score				> 0.999
<100	4 (50.0)	282 (55.9)	285	
≥ 100	4 (50.0)	222 (44.1)	226	

SISH, silver in situ hybridization; IHC, immunohistochemistry

Table 9. Clinicopathologic features of *MET* amplification and MET protein overexpression

	Amplification[1] n = 13 (3.8)	No amplification n = 325 (96.2)	p-value	Overexpression[2] n = 226 (44.2)	No overexpression n = 285 (55.8)	p-value
Age (yrs)			0.260			0.414
≤ 60	8 (61.5)	143 (44.0)		86 (38.1)	119 (41.8)	
> 60	5 (38.5)	182 (56.0)		140 (61.9)	166 (58.2)	
Gender			> 0.999			0.533
Male	7 (53.8)	171 (52.6)		111 (49.1)	149 (52.3)	
Female	6 (46.2)	158 (47.4)		115 (50.9)	136 (47.7)	
Smoking			> 0.999			0.161
Never	7 (53.8)	174 (53.5)		129 (57.1)	153 (53.7)	
Ex-	3 (23.1)	77 (23.7)		60 (26.5)	66 (23.2)	
Current	3 (23.1)	74 (22.8)		37 (16.4)	66 (23.2)	
Histology			0.028			0.012
ADC	9 (69.2)	282 (86.8)		205 (90.7)	240 (84.2)	
SCC	0 (0)	2 (0.6)		0 (0)	2 (0.7)	
MC	0 (0)	14 (4.3)		13 (5.8)	10 (3.5)	
SC	2 (15.4)	17 (5.2)		3 (1.3)	19 (6.7)	
LCC	2 (15.4)	8 (2.5)		3 (1.3)	9 (3.2)	
ASC	0 (0)	2 (0.6)		2 (0.9)	5 (1.8)	
CC	0 (0)	0 (0)		0 (0)	0 (0)	
CT	0 (0)	0 (0)		0 (0)	0 (0)	
Stage			0.014			< 0.001
I	2 (15.4)	172 (52.9)		153 (69.0)	147 (51.6)	
II	4 (30.8)	63 (19.4)		36 (15.9)	51 (17.9)	
III	6 (46.2)	79 (24.3)		28 (12.4)	74 (26.0)	
IV	1 (7.7)	11 (3.4)		6 (2.7)	13 (4.6)	

[1]*MET* amplification denotes a *MET/CEP17* ratio of ≥2.0 or an average *MET* copy number of ≥6.0 signals/cell.

[2]MET protein overexpression denotes an H-score of ≥100.

ADC, adenocarcinoma; ASC, adenosquamous carcinoma; CC, colloid adenocarcinoma; CT, carcinoid tumor; LCC, large cell carcinoma; MC, mucinous adenocarcinoma; SC, sarcomatoid carcinoma; SCC, squamous cell carcinoma

4. Survival analysis

*MET*ex14 showed a tendency of better OS and DFS. The *EGFR*-mutation group revealed significantly better OS and DFS compared with the wild type group (P<0.001 and P=0.027, respectively; Figure 7). Meanwhile, *MET* amplification showed poorer OS (P=0.188) and DFS (P=0.025). MET overexpression revealed better OS (P=0.023) and DFS (P<0.001).

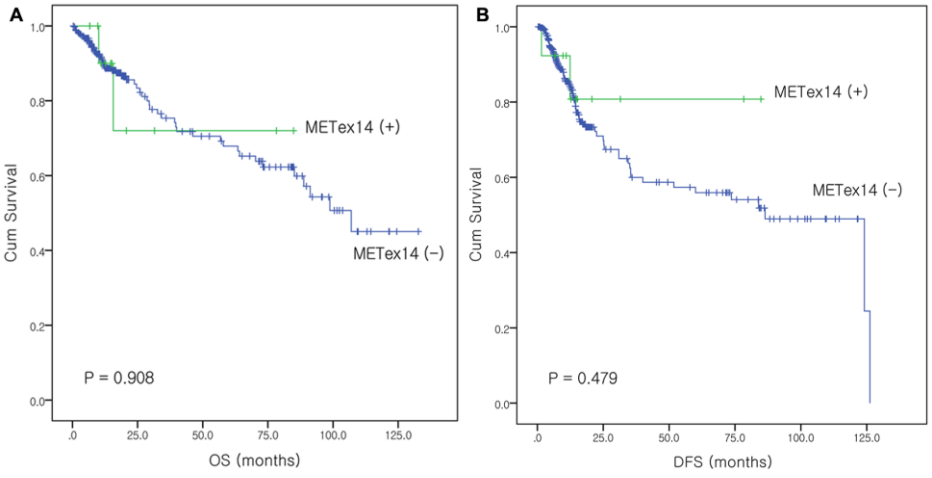

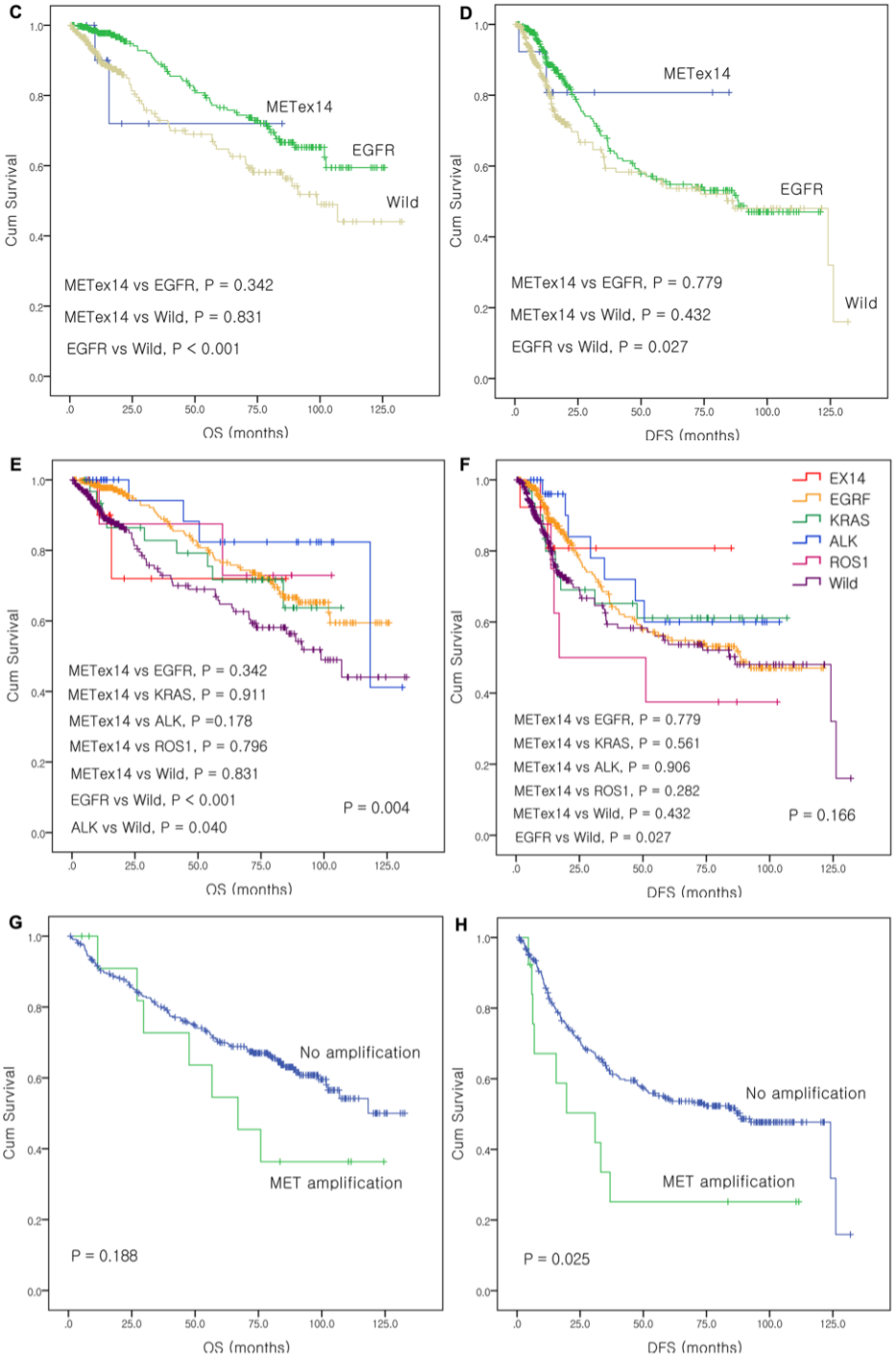

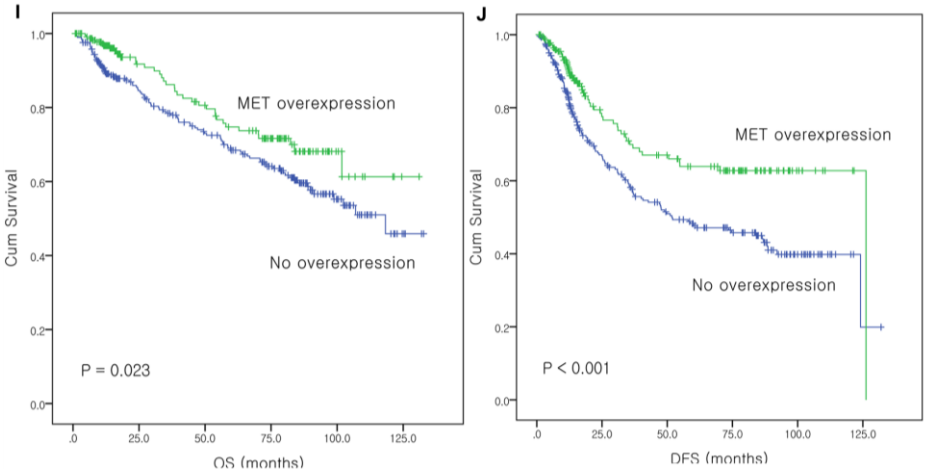

Figure 7. Kaplan–Meier curves of overall survival (OS) and disease free survival (DFS). A and B. The *MET*ex14-positive and *MET*ex14-negative groups show no differences in OS and DFS., C and D. *MET*ex14, *EGFR* mutation, and wild type. *EGFR*-mutation group shows significantly better OS and DFS than wild type group., E and F. *MET*ex14, *EGFR, KRAS, ALK,* and *ROS1* mutation, and wild type, The OS of each group is significantly different. G and H. The *MET*-amplified group shows poorer DFS than the non-amplified group., I and J. The MET overexpressed group shows better OS and DFS than the non-overexpressed group.

In the univariate Cox-poportional hazards models for OS (Table 10), old age, males, smokers, histology (SC), predominant subtype (solid and micropapillary), advanced stage, and wild type (non-*MET*ex14 and non-*EGFR* mutation) were associated with worse prognosis. Among them, old age, solid predominant pattern, and advanced stage were independent worse prognostic factors on multivariate analysis. In the univariate Cox-poportional hazards models for DFS (Table 11), histology (SC), non-lepidic subtype, advanced stage, and *MET* amplification were associated with worse prognosis. Among them, only advanced stage was an independent worse prognostic factor on multivariate analysis. MET overexpression showed better prognosis on univariate analysis for OS and DFS.

Table 10. Univariate and multivariate Cox-proportional hazards models for overall

survival

	Univariate analysis			Multivariate analysis		
	HR	95% CI	*P*	HR	95% CI	*P*
Age > 60 yrs.	1.423	1.011-2.003	0.043	1.531	1.007-2.327	0.046
Male	1.678	1.199-2.347	0.003	1.160	0.592-2.274	0.666
Smoking						
Never	1		0.004	1		0.357
Ex-	1.897	1.295-2.779	0.001	1.471	0.721-3.002	0.289
Current	1.377	0.909-2.085	0.131	1.006	0.481-2.103	0.987
Histology						
ADC	1		< 0.001	1		0.730
SCC	1.662	0.816-3.386	0.162	0.000	0.000-3.1E+249	0.970
MC	1.146	0.503-2.610	0.746	0.951	1.127-7.080	0.961
SC	5.576	2.985-10.415	<0.001	1.217	0.252-6.017	0.808
LCC	1.937	0.851-4.411	0.115	3.622	0.796-16.494	0.096
Other	1.503	0.208-10.888	0.408	0.000	0.000-2.5E+196	0.965
Subtype						
Lepidic	1		< 0.001	1		0.015
Acinar	1.347	0.613-2.963	0.459	1.679	0.511-5.515	0.393
Papillary	1.737	0.713-4.227	0.224	2.387	0.677-8.422	0.176
Solid	3.184	1.385-7.317	0.006	3.700	1.078-12.696	0.038
MP	3.550	1.471-8.572	0.005	2.939	0.803-10.750	0.103
Stage						
I	1		< 0.001	1		<0.001
II	3.267	2.076-5.143	< 0.001	3.081	1.682-5.644	<0.001
III	5.270	3.524-7.882	< 0.001	5.100	3.104-8.378	<0.001
IV	5.852	2.820-12.142	< 0.001	8.533	3.115-23.371	<0.001
Mutation						
*MET*ex14	1		0.001	1		0.774
EGFR	0.582	0.141-2.390	0.452	0.486	0.065-3.658	0.484
Wild	1.140	0.280-4.648	0.855	0.511	0.067-3.883	0.516
MET amplification	1.662	0.774-3.568	0.193	-		
MET over-expression	0.645	0.155-1.136	0.024	1.263	0.778-2.051	0.345

ADC, adenocarcinoma; HR, hazard ratio; CI, confidence interval; LCC, large cell carcinoma; MC, mucinous adenocarcinoma; MP, micropapillary; SC, sarcomatoid carcinoma; SCC, squamous cell carcinoma

Table 11. Univariate and multivariate Cox-proportional hazards models for disease free survival

	Univariate analysis			Multivariate analysis		
	HR	95% CI	*P*	HR	95% CI	*P*
Age > 60 yrs.	0.853	0.650-1.120	0.252	-		
Male	1.180	0.646-1.113	0.234	-		
Smoking						
Never	1		0.640	-		
Ex-	1.021	0.734-1.421	0.900			

Current	1.171	0.838-1.636	0.354			
Histology						
ADC	1		0.008	1		0.856
SCC	1.008	0.578-1.757	0.977	0.000	0.000-3.3E+194	0.962
MC	1.218	0.643-2.307	0.545	1.174	0.443-3.106	0.747
SC	3.105	1.753-5.501	<0.001	1.311	0.299-5.750	0.720
LCC	1.028	0.381-2.772	0.956	2.064	0.272-15.646	0.483
Other	1.750	0.431-7.107	0.434	3.406	0.441-26.321	0.240
Subtype						
Lepidic	1		<0.001	1		0.516
Acinar	2.052	1.033-4.074	0.040	1.106	0.503-2.432	0.802
Papillary	2.736	1.277-5.863	0.010	1.554	0.643-3.757	0.328
Solid	3.664	1.746-7.686	0.001	1.250	0.512-3.048	0.624
MP	5.099	2.357-11.032	<0.001	1.577	0.639-3.892	0.323
Stage						
I	1		<0.001	1		<0.001
II	3.601	2.473-5.243	<0.001	3.834	2.355-6.243	<0.001
III	6.802	4.857-9.527	<0.001	6.696	4.405-10.177	<0.001
IV	9.752	5.840-16.283	<0.001	8.473	3.852-18.639	<0.001
Mutation				-		
*MET*ex14	1		0.076			
EGFR	1.277	0.314-5.187	0.733			
Wild	1.765	0.435-7.160	0.427			
MET amplification	2.210	1.081-4.159	0.029	1.006	0.421-2.401	0.990
MET over-expression	0.564	0.408-0.778	<0.001	0.910	0.623-1.328	0.624

ADC, adenocarcinoma; HR, hazard ratio; CI, confidence interval; LCC, large cell carcinoma; MC, mucinous adenocarcinoma; MP, micropapillary; SC, sarcomatoid carcinoma; SCC, squamous cell carcinoma

5. Analysis of TCGA data and previous literature

Information from the *MET*ex14 cases obtained from the TCGA lung adenocarcinoma data (c-bioportal database; http://www.cbioportal.org) is presented in Table 12. The mean total mutation count in coding regions was 72.5. Of the retrieved cases, 53.8% (7/13) showed no co-mmutated oncogenic drivers and 23.1% (3/13) had a *TP53* mutation. *MET* amplification was found in one case. Amplification of *CDK4* and *MDM2* was observed in 54.5% (6/11) of the cases.

Table 12. *MET*ex14 data from The Cancer Genome Atlas

No.	Sample ID	*MET*ex14 alteration	Age	Gender	Smoking	Stage	OS/DFS (mo)	Total mutation burden	Other oncogenic mutation	Other oncogenic CNV
1	AU5884	c.3028+2T>C	64	Male	Ex-smoker	N/A	1.8	34	None	N/A
2	TCGA-49-6745-01	c.3028+1G>T	82	Male	Current	IIIA	4.9	124	*MGA* S947*, *SMAD2* D450N	*CDK4*, *MDM2*, *KRAS*, *GLI1* amplification *CDKN2A*, *CDKN2B*, *RAD51*, *MGA*, *TP53BP1*, *B2M* deep deletion
3	TCGA-50-5055-01	N/A	79	Female	N/A	IIA	25.8	21	None	*CDK4*, *MDM2* amplification
4	TCGA-44-6775-01	N/A	72	Female	Current	IB	2.7	71	*TP53* H168L, *NF1* E126*, *RB1* K616Ifs*37	*TP53*, *MAP2K4*, *NCOR1* deep deletion
5	TCGA-55-6978-01	N/A	81	Male	Never	IIA	5.5	38	None	*MET* amplification
6	TCGA-50-6597-01	c.3027_3028+2delAGGT	79	Female	Never	IB	33.3	60	*HLA-A* Q165*	*CDK4*, *MDM2*, *TERT*, *CCNE1*, *ERBB3*, *GLI1* amplification
7	TCGA-55-6982-01	c.3027_3028+4delAGGTAT	79	Female	Never	IIB	32.7	208	None	*CDK4*, *MDM2*, *TERT*, *GLI1* amplification
8	TCGA-75-5122-01	c.3028+2T>C	N/A	Male	Current	IB	N/A	125	None	*CDK4*, *MDM2*, *KRAS*, *TERT* amplification *PTPRD* deep deletion
9	TCGA-78-7143-01	c.2888-1G>A	62	Female	Never	IB	163.0	42	*TP53* R181H, *RB1* Q444Sfs*13	*MDM2*, *CARD11* amplification *BRCA1*, *PTPRD*, *RB1*, *LATS2* deep deletion
10	TCGA-93-7348-01	c.3028+1G>A	75	Female	Current	IA	4.2	99	*PIK3CA* E542K	*CDKN2A*, *CDKN2B* deep deletion
11	LUAD-NYU592-Tumor	c.3028+2T>C	N/A	Male	Current	IIIA	N/A	34	None	*CDK4*, *MDM2*, *CCND3*, *GLI1*, *VEGFA* amplification *CDKN2A*, *CDKN2B*, *KDM5C* deep deletion
12	TCGA-44-A47G-01	c.3028+2T>G	73	Female	Current	IA	4.4	76	*TP53* H193L	None

13	16640	c.2888-20_2889delTTCTTTCTCTCTGTTTTAAGAT	N/A	N/A	N/A	N/A	N/A	6	None	N/A

Table 13. *MET*ex14 data from previous literature

Ref.	Case No. (%)	Diagnostic method	Region	Histologic type	Age (median)	Gender (M:F)	Smoking (never:ever)	Stage	OS (multivariate)	MET overexpression	*MET* amplification	Mutation burden (/Mb)	Concurrent genomic alteration
5	7 (3.3)	RT-PCR followed by direct seq.	Japan	ADC	67	1:0.75	1:1.3	I	-	-	None	-	-
25	3 (3.4)	RNA (transcriptome) seq.	Korea	ADC	-	-	-	-	-	-	None	-	None
46	23 (1.3)	qRT-PCR	China	ADC (acinar)	67[1]	1:2[1]	1:0.2[1]	I[1]	-	Present[1]	Present	-	-
47	27 (3.3)	RT-PCR followed by direct seq.	Taiwan	ADC (solid)	77[1]	1:0.75	1:0.7	IV[1]	N/S	Present	-	-	-
48	18 (12.2)	qRT-PCR	Korea	ADC (acinar) SC	73[1]	1:2	1:1.1	I	-	Present	Present	-	-
30	5 (9.8)	NanoString-based multiplex fusion transcript analysis (RNA)	Korea	ADC	49	1:4	1:0.25	-	-	Present	None	-	*EGFR* ex19 del with T790M
49	18 (2.6)	Direct sequencing	Hong Kong	ADC SC	74	1:0.6	1:1	I, II	HR: 2.126[1]	Present[1]	Present[1]	-	-
50	12 (0.9)	Capture-based NGS (DNA), Direct seq. (RNA)	China	ADC	59	1:0.7	-	IV	-	Present	None	-	*KRAS* G12D
51	17 (2.1)	qRT-PCR followed by direct seq.	Korea	ADC (acinar)	73[1]	1:0.9	1:1.4	I	N/S	Present[1]	-	-	-
19	131 (3)	Hybrid capture based-NGS (DNA)	USA	ADC	-	-	-	-	-	-	Present	-	*TP53, PIK3CA; MDM2, CDK4, MYC, RET amp.*
52	8 (22.2)[b]	WES, RT-PCR followed by direct seq.	USA	SC[1]	79	1:1.7	1:7	I, II	-	-	-	3	*PIK3CA*

[18]	8 (-)	Hybrid capture based-NGS (DNA)	USA	ADC	77	1:1	1:1	IV	-	Present	Present	-	*TP53, DICER, TERT, BRCA1, MYC, PDGFRB, PIK3CA; MDM2, CDK4, MYC amp.*
[53]	28 (3.0)	Hybrid capture based-NGS (DNA) followed by qRT-PCR	USA	ADC SC	72.5[1]	1:2.1	1:1.8	I[1]	-	Present	Present	-	*TP53; MDM2*[1], *EGFR, CDK4,KRAS, ERRB3 amp.*
[54]	298 (2.7)	Hybrid capture based-CGP (DNA)	USA	ASC, SC, ADC (acinar)	73	1:1.5	1:0.4	IV	-	-	Present	Low (0-5)	*KRAS, EGFR, BRAF; ALK fusion; MDM2, CDK4, EGFR amp.*
[55]	12 (5.2)	PCR followed by direct seq.	France	ADC SC	67	1:1.4	1:2	-	-	-	Polysomy	-	*EGFR (G719A), KRAS (G12C)*
[56]	15 (12)[2]	CGP (DNA)	USA	SC	71	1:2	1:0.5	-	-	-	-	8.3	*TP53, CDKN2A, MLL2, SPTA1; PD-L1/L2, JAK2, CDK6, PIK3CG amp.*
[57]	26 (-)	Anchored multiplex RNA seq. followed by DNA seq.mO	USA	ADC	75	1:1.9	1:1.2	I	-	-	-	-	*PI3KCA, TP53, CTNNB, PTEN, CDKN2A, SMAD4*
[58]	5 (2)	Direct seq. followed by diverse commercial amplicon-based NGS panels (DNA)	France	ADC	80	1:0.7	0:3	-	-	-	-	-	-

[1]These results were statistically significant compared to other driver mutations and the wild type sequence in each study.

[2]These studies were conducted only on sarcomatoid carcinomas.

ADC, adenocarcinoma; ASC, adenosquamous carcinoma; CGP, comprehensive genomic profiling; HR, hazard ratio; N/S, not significant; SC, sarcomatoid carcinoma; WES, whole-exome sequencing

We also reviewed literature beyond the case report level. The results are summarized in Table 13. The most frequently used diagnostic method was RT-PCR followed by direct sequencing. Various NSG methods have been used, of which hybrid capture based-NGS (DNA) was used most frequently. The most common histologic type was adenocarcinoma, followed by sarcomatoid carcinoma. Acinar pattern was the most predominant subtype of adenocarcinoma. The patients were mainly elderly; some studies showed a statistically significant association with age[46-48, 51, 53]. While gender distribution varied among the studies, slightly more studies reported female predominance; this trend was, statistically significant in one study[46]. Smoking status was also different in each study, with a slightly higher percentage of ever smokers. On the other hand, one study that found a statistically significant association with never-smoker[46]. Excluding studies with stage IV patients only, several studies reported that *MET*ex14 NSCLC was often comprised of early stages, some of which were statistically significant[46, 53]. Multivariate analysis for OS was performed in three studies, one of which identified *MET*ex14 as an independent prognostic factor[49]. While the specific criteria differed from study to study, all studies with IHC reported MET overexpression, which was significantly associated with *MET*ex14 in some of the studies[46, 49, 51]. In some studies, concurrent *MET* amplification was present; this was statistically significant in one study[49]. Three studies evaluated the mutational tumor burden, which was shown to be relatively low at up to 8.3/Mb[52, 54, 56]. Concurrent genomic alteration was similar to that of TCGA, *TP53*, and *PIK3CA* mutations. *MDM2* and *CDK4* amplification were also repeated. A few cases were identified with actionable mutations in *EGFR* and *KRAS*[30, 50, 55]. To date, approximately equal numbers of studies have been performed on Asian versus Western cohorts with an average incidence of 3-4%. There was no significant difference between Asians and Westerners, but the patients tended to be older and to have relatively early stage cancer. Both ethnic groups showed some female predominance. Never-smokers tended to be slightly more prevalent in the Asian cohorts, while ever-smokers were slightly more prevalent in the Western cohorts.

IV. DISCUSSION

In NSCLC, it is becoming necessary to identify patients for targeted therapy. *MET*ex14 has been identified as a driver mutation in NSCLC; various therapeutic approaches have been attempted. In this study, we investigated the frequency of *MET*ex14 and the associated clinicopathologic features in Korean NSCLC cases. We also aimed to identify a suitable diagnostic approach for use in actual clinical settings.

To increase the sensitivity of *MET*ex14 detection, we first analyzed 414 *EGFR* mutation-negative adenocarcinomas by qRT-PCR. We also analyzed some of the *EGFR* mutation-negative adenocarcinomas by Sanger sequencing and pyrosequencing. Subsequently, NGS was performed for the cases that were positive by these tests. *MET*ex14 was found in 13 (3.1%) of these cases. Since the PCR probes used in this study were constructed by directly ligating the sequences of exons 13 and 15, the assay had 100% sensitivity to *MET*ex14. One case (case #14) showed a mismatch result, with the oncogenic mutation *KRAS* Q61H instead of *MET*ex14 as detected by NGS. In the two cases where a deletion was found only by pyrosequencing, NGS revealed a wild sequence and an *EGFR* L858R mutation. In these three cases, the VAF of RNA sequencing showing exon 14 loss was 0.06% (30/51712), 0.04% (3/6824), and 0.08% (8/9837). Although definitive criteria for VAF have not been established, we conclud that the VAF of the latter two cases, in which *MET*ex14 was not detected by RT-PCR, and the VAF of case #14 are not significantly different from each other. However, DNA sequencing of case #14 revealed a missense mutation (exon 17; c.G3509A; VAF 4%) and a frameshift insertion (exon 21; c.4017_4018insTT; VAF 3%) at positions corresponding to the tyrosine kinase domain of MET. *MET* p.R1170Q (c.G3509A) has been reported to be a pathogenic mutation, but only in malignant melanoma[59]. In addition, single base substitutions of intron sites other than introns 13 and 14 have also been found. *MET*ex14 has only been reported to be caused by mutations in regions around exon 14. Therefore, additional studies are needed to determine whether *MET*ex14 can be induced at other sites (i.e. not around exon 14).

Sanger sequencing had no false-positive result (100% specificity), but the false negative rate was relatively high. Five cases without observed mutations were actually found to have *MET*ex14 on NGS. These cases had either large deletions or small numbers of supporting DNA reads, which thus could not be detected due to the limitations of the Sanger sequencing test itself. Pyrosequencing showed poor performance for detecting *MET*ex14 with low sensitivity and low specificity. A limitation of pyrosequencing is that it is difficult to detect the de novo sequence. Moreover, read length is restricted and the optimal sequencing primer must be used. Considering the sensitivity, specificity, reproducibility, detection limit, turnaround time, ease of interpretation, and cost of the different assays, we suggest that qRT-PCR is the most reasonable clinical testing platform for detecting *MET*ex14. To our knowledge, this is the first study to conduct a comparative analysis of the different diagnostic platforms for *MET*ex14.

Previous studies have used diverse types of NGS including whole-exome sequencing (WES)[2, 52], anchored multiplex RNA sequencing[57], and hybrid capture NGS[18, 19, 53]. We used hybrid capture targeted DNA/RNA sequencing methods. DNA sequencing revealed various lengths of indel around and in exon 14. Since genomic alterations of *MET*ex14 are very diverse, proper probes (for the hybrid-capture method) or primers (for the amplicon-based method) targeting exon 14 and its surrounding introns should be employed in DNA-NGS. In our study, with RNA sequencing, it was much easier to find out *MET*ex14 using the integrative genomics viewer (IGV), and the mean supporting read (%) was higher than with DNA sequencing. The higher supporting reads and higher VAF in RNA sequencing can be explained the following. Generally, extracted DNAs come from various cells, including nonneoplastic cells (such as inflammatory cells and stromal cells) and neoplastic cells. Wild-type DNAs from normal cells reduce the proportion of mutant DNA. On the other hand, mRNAs are extracted only from cells expressing MET mRNA. Since not all normal cells undergo *MET* transcription, the proportion of spliced RNA increases compared with genomic DNA. Although RNA handling in FFPE tissue can be complicated and less manageable than using DNA, it is a good method for novel transcripts, fusions, or

detection of allele-specific expression and identification of alternatively spliced genes[60, 61]. In general, the frequencies of DNA and RNA mutation alleles are highly correlated, and mutations are transcribed at a rate equivalent to the DNA allele frequency[62]. However, in some studies, mutant-biased transcriptional upregulation has been observed for some missense single nucleotide variants (SNVs), such as those on *EGFR* and *KRAS*[63, 64]. A recent study of the distribution of allelic fraction difference (AFD) (RNA-VAF minus DNA-VAF) in various tumor types reported a bias between the DNA- and RNA-VAFs. The AFD biases were notable for the nonsense SNVs and frameshift indels toward negative AFD (RNA-VAF < DNA-VAF) and for the splice site mutations toward positive AFD (RNA-VAF > DNA-VAF)[65]. Similar results (i.e. positive AFD) were seen with *MET*ex14, suggesting that *MET*ex14 may be subject to different transcriptional or posttranscriptional regulation leading to the observed allelic fraction difference.

We did not observe any correlations between *MET*ex14, *MET* amplification, and protein overexpression. Although *MET*ex14 and MET overexpression have been reported to be present together, there are no established IHC criteria for MET overexpression. In addition, the extent of observed correlation between *MET* amplification and protein overexpression varies between studies. In a profiling analysis, MET protein expression was detected in 65% of all lung adenocarcinomas, while only 10% of the MET-positive tumors (as assessed by immunohistochemistry) harbored *MET* DNA alterations. This finding suggests that a different biological mechanism is responsible for inducing MET protein expression[4]. A common mechanism of MET activation in cancer is protein overexpression, which results mainly from transcriptional upregulation by a variety of factors[66]. In addition, intratumoral heterogeneity in MET expression has been described[48]. Therefore, MET overexpression as assessed by IHC may not be suitable for screening for *MET*ex14 or *MET* amplification[38, 67]. Although many studies have suggested that MET overexpression is associated with poor prognosis[68], this study showed that MET overexpression is associated with good prognosis by univariate survival analysis. This finding could be explained by the fact that most of the MET-overexpressing NSCLCs in the cohort were

concentrated in the early stages ($p<0.001$). Moreover MET overexpression was not significant in the multivariate analysis. Many studies have reported that *MET* amplification is associated with advanced stage, undifferentiated pathological grade, and shorter OS[13, 49]. Here, *MET* amplification was associated with advanced stage and LCCs or SCs and was a poor prognostic factor on univariate analysis. Although concurrent *MET* amplification with *MET*ex14 was not detected by NGS or SISH in this study, this phenomenon has been identified in up to about 30% of cases[49, 54]. In these cases, poor histologic differentiation and relatively high mutational burden have been reported[54], supporting that *MET*ex14 is an early event of lung tumorigenesis, followed by *MET* amplification, resulting in a more aggressive clinical feature[53].

The Cancer Genome Atlas shows that any remarkable driver mutations other than *TP53*, but *CDK4* and *MDM2* amplification was relatively not uncommon, similar to the findings of other studies[18, 54, 69]. In this study, well-known oncogenic mutations or copy number variation were not observed except for *TP53* mutation in two cases. *MYC* T73P were observed in 69.2% (9/13) of cases, which is unusual. Although *MYC* T73P is known to be oncogenic, its significance in NSCLC remains unclear. Together with the results of recent researches, *MET*ex14 is likely to act as an oncogenic driver.

Compared with the *EGFR*, *KRAS*, *ALK* and *ROS1* mutation group and all-negative group, the *MET*ex14 group showed characteristic clinicopathologic features. *MET*ex14 was associated with old age, lepidic predominant pattern, and early stage. Compared with the *EGFR*, *ALK*, and *ROS1* mutant group, the *MET*ex14 group showed that *MET*ex14 was more frequent in males; however, compared with the *KRAS* mutant group and all-negative group, the *MET*ex14 group showed that *MET*ex14 was more common in females. *MET*ex14 was also more frequent with never smokers, compared with the *KRAS* and *ALK* mutant group and all-negative group. In our cohort, *MET*ex14 was found in ADC (4.8%; 11/230) and SC (9.5%; 2/21) histology only. In previous studies, *MET*ex14 was found frequently in SCs, and our data showed similar results[48, 52, 55, 56]. Ethnic differences in oncogenic mutations such as *EGFR* and *KRAS* are well known.

Comparing studies of Asian and Western cohorts, the frequency of *MET*ex14 was 3-4%, and was not significantly different in the cohorts. Older age, early stage, and slight female predominance were not significantly different in terms of geographical regions. The number of never smokers tended to be slightly higher in Asians, while the number of ever smokers was higher in Westerners. However, this is somewhat different from the recent study comparing the Japanese cohort with the TCGA (USA) data[70], and further studies are needed with regard to clinicopathologic features, with no systematic comparisons of race to date. One study suggested that a relatively low mutational burden of *MET*ex14 might be associated with a higher proportion of never smokers[54].

We observed moderate to marked lymphocytic infiltration in 53.8% of *MET*ex14 NSCLCs as an additional histologic feature. A recent retrospective analysis of the immunophenotypes of *MET*ex14 NSCLC revealed that PD-L1 expression (≥ 50%) was observed in 44% (18/41) of cases. However, the overall response rate to immunotherapy was only 13%[71]. Thus, more investigations are needed to understand the interaction of *MET* with immune checkpoint pathways.

Each study has shown a difference in the prognostic relevance of *MET*ex14. We found that *MET*ex14 had a relatively good OS and a low hazard ratio in patients who underwent complete surgical resection. This is thought to be mainly affected by the early stages. In advanced stage, *MET*ex14 and *MET* amplification are relatively good predictors of response to MET-targeting therapies, providing the basis for screening patients with *MET*ex14 - particularly for elderly patients with ADC or SC histology.

V. CONCLUSION

In summary, this comparative study of molecular diagnostic assays showed that qRT-PCR, an mRNA-based method, is a sensitive and specific test and can be a good single gene test to screen *MET*ex14. A classic DNA-based method is possible; however, sensitivity can be hampered by large deletions of the *MET* gene or low allele frequency. If NGS is available, the gene panel should be designed to cover the genomic complexity of the *MET* gene. *MET*ex14 occurs in about 3% of

NSCLCs and has characteristic clinicopathologic features.

REFERENCES

1. Pao W, Girard N. New driver mutations in non-small-cell lung cancer. The Lancet Oncology. 2011;12:175-80.
2. Comprehensive molecular profiling of lung adenocarcinoma. Nature. 2014;511:543-50.
3. Kris MG, Johnson BE, Berry LD, Kwiatkowski DJ, Iafrate AJ, Wistuba, II, et al. Using multiplexed assays of oncogenic drivers in lung cancers to select targeted drugs. Jama. 2014;311:1998-2006.
4. Yeung SF, Tong JH, Law PP, Chung LY, Lung RW, Tong CY, et al. Profiling of Oncogenic Driver Events in Lung Adenocarcinoma Revealed MET Mutation as Independent Prognostic Factor. Journal of thoracic oncology : official publication of the International Association for the Study of Lung Cancer. 2015;10:1292-300.
5. Onozato R, Kosaka T, Kuwano H, Sekido Y, Yatabe Y, Mitsudomi T. Activation of MET by gene amplification or by splice mutations deleting the juxtamembrane domain in primary resected lung cancers. Journal of thoracic oncology : official publication of the International Association for the Study of Lung Cancer. 2009;4:5-11.
6. Comprehensive genomic characterization of squamous cell lung cancers. Nature. 2012;489:519-25.
7. Chatziandreou I, Tsioli P, Sakellariou S, Mourkioti I, Giannopoulou I, Levidou G, et al. Comprehensive Molecular Analysis of NSCLC; Clinicopathological Associations. PloS one. 2015;10:e0133859.
8. Petrini I. Biology of MET: a double life between normal tissue repair and tumor progression. Annals of translational medicine. 2015;3:82.
9. Peruzzi B, Bottaro DP. Targeting the c-Met signaling pathway in cancer. Clinical cancer research : an official journal of the American Association for Cancer Research. 2006;12:3657-60.
10. Engelman JA, Zejnullahu K, Mitsudomi T, Song Y, Hyland C, Park JO, et al. MET amplification leads to gefitinib resistance in lung cancer by activating ERBB3 signaling. Science (New York, NY). 2007;316:1039-43.

11. Engelman JA JnP. Mechanisms of acquired resistance to epidermal growth factor receptor tyrosine kinase inhibitors in non-small cell lung cancer. Clinical cancer research : an official journal of the American Association for Cancer Research. 2008;14:2895-9.

12. Okuda K, Sasaki H, Yukiue H, Yano M, Fujii Y. Met gene copy number predicts the prognosis for completely resected non-small cell lung cancer. Cancer science. 2008;99:2280-5.

13. Cappuzzo F, Marchetti A, Skokan M, Rossi E, Gajapathy S, Felicioni L, et al. Increased MET gene copy number negatively affects survival of surgically resected non-small-cell lung cancer patients. Journal of clinical oncology : official journal of the American Society of Clinical Oncology. 2009;27:1667-74.

14. Camidge DR OS, Shapiro G, Otterson GA, Villaruz LC, Villalona-Calero MA, et al. . Efficacy and safety of crizotinib in patients with advanced c-MET-amplified non-small cell lung cancer (NSCLC). Journal of clinical oncology : official journal of the American Society of Clinical Oncology. 2014 32:5s, 2014 (suppl; abstr 8001).

15. Spigel DR, Edelman MJ, Mok T, O'Byrne K, Paz-Ares L, Yu W, et al. Treatment Rationale Study Design for the MetLung Trial: A Randomized, Double-Blind Phase III Study of Onartuzumab (MetMAb) in Combination With Erlotinib Versus Erlotinib Alone in Patients Who Have Received Standard Chemotherapy for Stage IIIB or IV Met-Positive Non-Small-Cell Lung Cancer. Clinical lung cancer. 2012;13:500-4.

16. Scagliotti GV NS, Schiller JH , Hirsh V , Sequist LV , Soria JC , et al. Rationale and design of MARQUEE: a phase III, randomized, double-blind study of tivantinib plus erlotinib versus placebo plus erlotinib in previously treated patients with locally advanced or meta-static, nonsquamous, non–small cell lung cancer. Clinical lung cancer. 2012 13:391 – 5.

17. David R. Spigel TJE, Rodryg A. Ramlau et al. . Randomized Phase II Trial of Onartuzumab in Combination With Erlotinib in Patients With Advanced Non–Small-Cell Lung Cancer. J Clin Oncol. 2013;31:4105–14.

18. Paik PK, Drilon A, Yu H, Rekhtman N, Ginsberg MS, Borsu L, et al.

Response to MET inhibitors in patients with stage IV lung adenocarcinomas harboring MET mutations causing exon 14 skipping. Cancer discovery. 2015.
19. Frampton GM, Ali SM, Rosenzweig M, Chmielecki J, Lu X, Bauer TM, et al. Activation of MET via diverse exon 14 splicing alterations occurs in multiple tumor types and confers clinical sensitivity to MET inhibitors. Cancer discovery. 2015.
20. Ma PC, Kijima T, Maulik G, Fox EA, Sattler M, Griffin JD, et al. c-MET mutational analysis in small cell lung cancer: novel juxtamembrane domain mutations regulating cytoskeletal functions. Cancer research. 2003;63:6272-81.
21. Ma PC, Jagadeeswaran R, Jagadeesh S, Tretiakova MS, Nallasura V, Fox EA, et al. Functional expression and mutations of c-Met and its therapeutic inhibition with SU11274 and small interfering RNA in non-small cell lung cancer. Cancer research. 2005;65:1479-88.
22. Kong-Beltran M, Seshagiri S, Zha J, Zhu W, Bhawe K, Mendoza N, et al. Somatic mutations lead to an oncogenic deletion of met in lung cancer. Cancer research. 2006;66:283-9.
23. Lee JM, Kim B, Lee SB, Jeong Y, Oh YM, Song YJ, et al. Cbl-independent degradation of Met: ways to avoid agonism of bivalent Met-targeting antibody. Oncogene. 2014;33:34-43.
24. Ma PC. MET Receptor Juxtamembrane Exon 14 Alternative Spliced Variant: Novel Cancer Genomic Predictive Biomarker. Cancer discovery. 2015;5:802-5.
25. Seo JS, Ju YS, Lee WC, Shin JY, Lee JK, Bleazard T, et al. The transcriptional landscape and mutational profile of lung adenocarcinoma. Genome research. 2012;22:2109-19.
26. IARC. WHO classification of tumors of the lung, pleura, thymus, and heart. Lyon, France: IARC Press; 2015.
27. Goldstraw P, Crowley J, Chansky K, Giroux DJ, Groome PA, Rami-Porta R, et al. The IASLC Lung Cancer Staging Project: proposals for the revision of the TNM stage groupings in the forthcoming (seventh) edition of the TNM Classification of malignant tumours. Journal of thoracic oncology : official publication of the International Association for the Study of Lung Cancer.

2007;2:706-14.
28. Greene FL, American Joint Committee on C, American Cancer S. AJCC cancer staging manual. New York :: Springer-Verlag; 2010.
29. Sun S, Schiller JH, Gazdar AF. Lung cancer in never smokers--a different disease. Nature reviews Cancer. 2007;7:778-90.
30. Lee J, Ou SH, Lee JM, Kim HC, Hong M, Kim SY, et al. Gastrointestinal malignancies harbor actionable MET exon 14 deletions. Oncotarget. 2015;6:28211-22.
31. Li H, Durbin R. Fast and accurate short read alignment with Burrows-Wheeler transform. Bioinformatics (Oxford, England). 2009;25:1754-60.
32. Dobin A, Davis CA, Schlesinger F, Drenkow J, Zaleski C, Jha S, et al. STAR: ultrafast universal RNA-seq aligner. Bioinformatics (Oxford, England). 2013;29:15-21.
33. Haas B, Dobin A, Stransky N, Li B, Yang X, Tickle T, et al. STAR-Fusion: Fast and Accurate Fusion Transcript Detection from RNA-Seq. bioRxiv. 2017.
34. Nicorici D, Satalan M, Edgren H, Kangaspeska S, Murumagi A, Kallioniemi O, et al. FusionCatcher - a tool for finding somatic fusion genes in paired-end RNA-sequencing data. bioRxiv. 2014.
35. Pertea M, Kim D, Pertea GM, Leek JT, Salzberg SL. Transcript-level expression analysis of RNA-seq experiments with HISAT, StringTie and Ballgown. Nature protocols. 2016;11:1650-67.
36. Robinson MD, McCarthy DJ, Smyth GK. edgeR: a Bioconductor package for differential expression analysis of digital gene expression data. Bioinformatics (Oxford, England). 2010;26:139-40.
37. Dietel M, Ellis IO, Hofler H, Kreipe H, Moch H, Dankof A, et al. Comparison of automated silver enhanced in situ hybridisation (SISH) and fluorescence ISH (FISH) for the validation of HER2 gene status in breast carcinoma according to the guidelines of the American Society of Clinical Oncology and the College of American Pathologists. Virchows Archiv : an international journal of pathology. 2007;451:19-25.
38. Jurmeister P, Lenze D, Berg E, Mende S, Schaper F, Kellner U, et al. Parallel

screening for ALK, MET and ROS1 alterations in non-small cell lung cancer with implications for daily routine testing. Lung cancer (Amsterdam, Netherlands). 2015;87:122-9.

39. Rogers TM, Russell PA, Wright G, Wainer Z, Pang JM, Henricksen LA, et al. Comparison of methods in the detection of ALK and ROS1 rearrangements in lung cancer. Journal of thoracic oncology : official publication of the International Association for the Study of Lung Cancer. 2015;10:611-8.

40. Kim HJ, Lee KY, Kim YC, Kim KS, Lee SY, Jang TW, et al. Detection and comparison of peptide nucleic acid-mediated real-time polymerase chain reaction clamping and direct gene sequencing for epidermal growth factor receptor mutations in patients with non-small cell lung cancer. Lung cancer (Amsterdam, Netherlands). 2012;75:321-5.

41. Han HS, Lim SN, An JY, Lee KM, Choe KH, Lee KH, et al. Detection of EGFR mutation status in lung adenocarcinoma specimens with different proportions of tumor cells using two methods of differential sensitivity. Journal of thoracic oncology : official publication of the International Association for the Study of Lung Cancer. 2012;7:355-64.

42. Paik JH, Choi CM, Kim H, Jang SJ, Choe G, Kim DK, et al. Clinicopathologic implication of ALK rearrangement in surgically resected lung cancer: a proposal of diagnostic algorithm for ALK-rearranged adenocarcinoma. Lung cancer (Amsterdam, Netherlands). 2012;76:403-9.

43. Go H, Kim DW, Kim D, Keam B, Kim TM, Lee SH, et al. Clinicopathologic analysis of ROS1-rearranged non-small-cell lung cancer and proposal of a diagnostic algorithm. Journal of thoracic oncology : official publication of the International Association for the Study of Lung Cancer. 2013;8:1445-50.

44. Cerami E, Gao J, Dogrusoz U, Gross BE, Sumer SO, Aksoy BA, et al. The cBio cancer genomics portal: an open platform for exploring multidimensional cancer genomics data. Cancer discovery. 2012;2:401-4.

45. Gao J, Aksoy BA, Dogrusoz U, Dresdner G, Gross B, Sumer SO, et al. Integrative analysis of complex cancer genomics and clinical profiles using the cBioPortal. Science signaling. 2013;6:pl1.

46. Zheng D, Wang R, Ye T, Yu S, Hu H, Shen X, et al. MET exon 14 skipping defines a unique molecular class of non-small cell lung cancer. Oncotarget. 2016;7:41691-702.
47. Gow CH, Hsieh MS, Wu SG, Shih JY. A comprehensive analysis of clinical outcomes in lung cancer patients harboring a MET exon 14 skipping mutation compared to other driver mutations in an East Asian population. Lung cancer (Amsterdam, Netherlands). 2017;103:82-9.
48. Kwon D, Koh J, Kim S, Go H, Kim YA, Keam B, et al. MET exon 14 skipping mutation in triple-negative pulmonary adenocarcinomas and pleomorphic carcinomas: An analysis of intratumoral MET status heterogeneity and clinicopathological characteristics. Lung cancer (Amsterdam, Netherlands). 2017;106:131-7.
49. Tong JH, Yeung SF, Chan AW, Chung LY, Chau SL, Lung RW, et al. MET Amplification and Exon 14 Splice Site Mutation Define Unique Molecular Subgroups of Non-Small Cell Lung Carcinoma with Poor Prognosis. Clinical cancer research : an official journal of the American Association for Cancer Research. 2016;22:3048-56.
50. Liu SY, Gou LY, Li AN, Lou NN, Gao HF, Su J, et al. The Unique Characteristics of MET Exon 14 Mutation in Chinese Patients with NSCLC. Journal of thoracic oncology : official publication of the International Association for the Study of Lung Cancer. 2016;11:1503-10.
51. Lee GD, Lee SE, Oh DY, Yu DB, Jeong HM, Kim J, et al. MET Exon 14 Skipping Mutations in Lung Adenocarcinoma: Clinicopathologic Implications and Prognostic Values. Journal of thoracic oncology : official publication of the International Association for the Study of Lung Cancer. 2017;12:1233-46.
52. Liu X, Jia Y, Stoopler MB, Shen Y, Cheng H, Chen J, et al. Next-Generation Sequencing of Pulmonary Sarcomatoid Carcinoma Reveals High Frequency of Actionable MET Gene Mutations. Journal of clinical oncology : official journal of the American Society of Clinical Oncology. 2015.
53. Awad MM, Oxnard GR, Jackman DM, Savukoski DO, Hall D, Shivdasani P, et al. MET Exon 14 Mutations in Non-Small-Cell Lung Cancer Are Associated

With Advanced Age and Stage-Dependent MET Genomic Amplification and c-Met Overexpression. Journal of clinical oncology : official journal of the American Society of Clinical Oncology. 2016;34:721-30.

54. Schrock AB, Frampton GM, Suh J, Chalmers ZR, Rosenzweig M, Erlich RL, et al. Characterization of 298 Patients with Lung Cancer Harboring MET Exon 14 Skipping Alterations. Journal of thoracic oncology : official publication of the International Association for the Study of Lung Cancer. 2016;11:1493-502.

55. Saffroy R, Fallet V, Girard N, Mazieres J, Moro Sibilot D, Lantuejoul S, et al. MET exon 14 mutations as targets in routine molecular analysis of primary sarcomatoid carcinoma of the lung. Oncotarget. 2017.

56. Schrock AB, Li SD, Frampton GM, Suh J, Braun E, Mehra R, et al. Pulmonary sarcomatoid carcinomas commonly harbor either potentially targetable genomic alterations or high tumor mutational burden as observed by comprehensive genomic profiling. Journal of thoracic oncology : official publication of the International Association for the Study of Lung Cancer. 2017.

57. Heist RS, Shim HS, Gingipally S, Mino-Kenudson M, Le L, Gainor JF, et al. MET Exon 14 Skipping in Non-Small Cell Lung Cancer. The oncologist. 2016;21:481-6.

58. Poirot B, Doucet L, Benhenda S, Champ J, Meignin V, Lehmann-Che J. Brief report: MET exon 14 alterations and new resistance-mutations to tyrosine kinase inhibitors: risk of inadequate detection with current amplicon-based NGS panels. Journal of thoracic oncology : official publication of the International Association for the Study of Lung Cancer. 2017.

59. Prickett TD, Agrawal NS, Wei X, Yates KE, Lin JC, Wunderlich JR, et al. Analysis of the tyrosine kinome in melanoma reveals recurrent mutations in ERBB4. Nature genetics. 2009;41:1127-32.

60. Ozsolak F, Milos PM. RNA sequencing: advances, challenges and opportunities. Nat Rev Genet. 2011;12:87-98.

61. Mercer TR, Clark MB, Crawford J, Brunck ME, Gerhardt DJ, Taft RJ, et al. Targeted sequencing for gene discovery and quantification using RNA CaptureSeq. Nat Protocols. 2014;9:989-1009.

62. Castle JC, Loewer M, Boegel S, Tadmor AD, Boisguerin V, de Graaf J, et al. Mutated tumor alleles are expressed according to their DNA frequency. Scientific reports. 2014;4:4743.
63. Govindan R, Ding L, Griffith M, Subramanian J, Dees ND, Kanchi KL, et al. Genomic landscape of non-small cell lung cancer in smokers and never-smokers. Cell. 2012;150:1121-34.
64. Mayba O, Gilbert HN, Liu J, Haverty PM, Jhunjhunwala S, Jiang Z, et al. MBASED: allele-specific expression detection in cancer tissues and cell lines. Genome biology. 2014;15:405.
65. Rhee JK, Lee S, Park WY, Kim YH, Kim TM. Allelic imbalance of somatic mutations in cancer genomes and transcriptomes. Scientific reports. 2017;7:1653.
66. Organ SL, Tsao MS. An overview of the c-MET signaling pathway. Therapeutic advances in medical oncology. 2011;3:S7-s19.
67. Watermann I, Schmitt B, Stellmacher F, Muller J, Gaber R, Kugler C, et al. Improved diagnostics targeting c-MET in non-small cell lung cancer: expression, amplification and activation? Diagnostic pathology. 2015;10:130.
68. Guo B, Cen H, Tan X, Liu W, Ke Q. Prognostic value of MET gene copy number and protein expression in patients with surgically resected non-small cell lung cancer: a meta-analysis of published literatures. PloS one. 2014;9:e99399.
69. Awad MM. Impaired c-Met Receptor Degradation Mediated by MET Exon 14 Mutations in Non-Small-Cell Lung Cancer. Journal of clinical oncology : official journal of the American Society of Clinical Oncology. 2016;34:879-81.
70. Saito M, Shiraishi K, Kunitoh H, Takenoshita S, Yokota J, Kohno T. Gene aberrations for precision medicine against lung adenocarcinoma. Cancer science. 2016;107:713-20.
71. Sabari JK, Montecalvo J, Chen R, Dienstag JA, Mrad C, Bergagnini I, et al. PD-L1 expression and response to immunotherapy in patients with MET exon 14-altered non-small cell lung cancers (NSCLC). Journal of Clinical Oncology. 2017;35:8512-.

ABSTRACT (IN KOREAN)

비소세포폐암에서 *MET* 엑손 14번 스키핑 돌연변이; 진단적 접근법과 임상병리학적 의의

<지도교수 심 효 섭>

연세대학교 대학원 의학과

김 은 경

비소세포폐암의 발암 유전자 중 하나로 알려진 *MET* 엑손 14 스키핑 돌연변이는 MET 억제제의 반응을 예측할 수 있는 바이오마커로써, 이 변이를 표적 치료를 위한 환자 선택 과정에 포함시키는 것이 중요해지고 있다. 그러나 *MET* 엑손 14 스키핑은 매우 다양한 유전적 변이로 나타나기 때문에 진단적으로 어려운 문제가 될 수 있다. 따라서 이 연구에서는 *MET* 엑손 14 스키핑 돌연변이의 합리적인 진단적 접근법을 찾고, *MET* 유전자 증폭 및 단백질 과발현을 비롯한 다른 유전적 변이와의 관련성을 확인하고자 하였다. 또한 한국인 비소세포폐암에서 *MET* 엑손 14 스키핑의 임상 병리학적 특징을 확인하였다. *EGFR* / *KRAS* 돌연변이 음성 및 *ALK* / *ROS1* 재배열 음성 (4중 음성)인 414개의 외과적으로 절제된 비소세포폐암 조직으로 *MET* 엑손 14 스키핑을 포괄적으로 분석하였다. 첫 단계로 실시간 정량 역전사 중합효소 연쇄 반응 (Real time qRT-PCR), 생어 염기서열 분석 및 파이로시퀀싱을 사용했으며, 이 중 하나 이상의 검사에서 양성 반응을 보인 경우, 차세대 염기서열분석 (NGS, hybrid capture targeted DNA / RNA 염기서열분석)을 시행하였다. 총 880개의 비소세포폐암군에서 *MET* 엑손 14 스키핑군의 임상병리학적 의의를 분석하였다. 차세대 염기서열분석을 통해 *MET* 엑손 14 스키핑은 13 명 (3.1 %)이 확인되었다. 첫 번째와 두 번째 단계의

결과를 비교할 때, 역전사 중합효소 연쇄 반응의 일치율이 가장 높았다. 평균 변이 빈도는 DNA-NGS와 RNA-NGS 분석에서 각각 10.5 % 및 49 % 였다. DNA-NGS에서 다양한 길이의 삽입, 결실, 및 치환이 엑손 14 주변과 내부에서 나타났다. 또한 *MET* 엑손 14 스키핑은 선암종/육종양암, 고령, 비흡연자, 초기 병기 등과 관련이 있었다. 두 개의 증례에서 나타난 *TP53* 돌연변이 이외에는 발암 유전자 돌연변이 또는 복제수 변이가 발견되지 않았다. *MET* 유전자 증폭은 관찰되지 않았고, 절반의 경우는 MET 단백질 과발현을 보였다. 요약하면, *MET* 엑손 14 스키핑 돌연변이는 비소세포폐암의 약 3 % 에서 발생하며 특징적인 임상 병리학적 특징을 갖는다. *MET* 엑손 14 스키핑 돌연변이를 검출하기 위해서는 고전적인 DNA 기반의 방법도 가능하지만, 큰 결실과 낮은 변이 빈도를 보일 경우 민감도가 떨어질 수 있다. mRNA 기반의 역전사 중합효소 연쇄 반응은 *MET* 엑손 14 스키핑 돌연변이에 대한 선별 목적으로 적절한 민감도와 특이도를 보인다. 다중 패널 염기서열분석을 이용할 경우에는 유전자 패널은 *MET*ex14를 검출하기 위해 *MET* 유전자의 복잡성을 포괄하도록 설계 되어야 한다.

핵심되는 말 : *MET* 엑손 14 스키핑, *MET* 증폭, MET 단백질 과발현, 비소세포폐암, 역전사 중합효소 연쇄 반응, 생어 염기서열 분석, 파이로시퀀싱, 차세대 염기서열분석